

SpatialVID: A Large-Scale Video Dataset with Spatial Annotations

Jiahao Wang^{1†} Yufeng Yuan^{1†} Rujie Zheng^{1†} Youtian Lin¹ Jian Gao¹
 Lin-Zhuo Chen¹ Yajie Bao¹ Yi Zhang¹ Chang Zeng¹ Yanxi Zhou¹
 Xiao-Xiao Long¹ Hao Zhu¹ Zhaoxiang Zhang² Xun Cao¹ Yao Yao^{1‡}

¹Nanjing University ²Institute of Automation, Chinese Academy of Sciences [†]Equal contribution [‡]Corresponding author

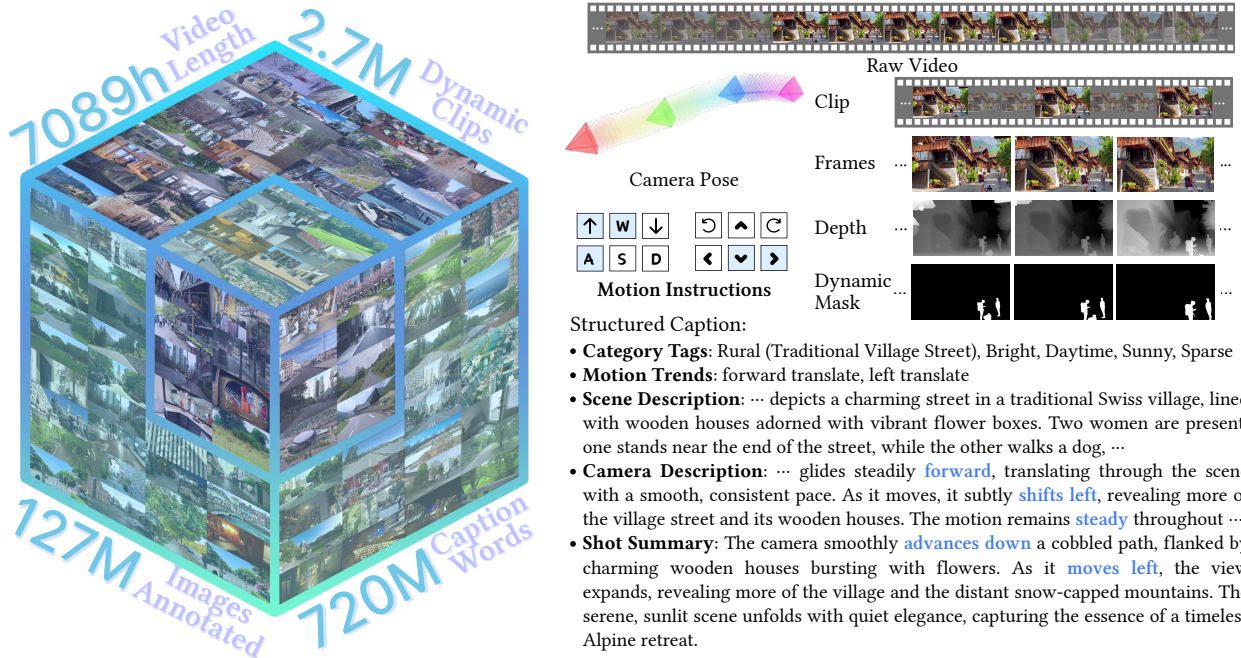


Figure 1. We introduce SpatialVID, a large-scale video dataset with explicit spatial annotations including camera poses, depth maps, structured captions and serialized motion instructions. The dataset consists of 7,089 hours of real-world dynamic scenes. An exemplar of our SpatialVID is shown on the right.

Abstract

Significant progress has been made in spatial intelligence, spanning both spatial reconstruction and world exploration. However, the scalability and real-world fidelity of current models remain severely constrained by the scarcity of large-scale, high-quality training data. While several datasets provide camera pose information, they are typically limited in scale, diversity, and annotation richness, particularly for real-world dynamic scenes with ground-truth camera motion. To this end, we collect **SpatialVID**, a dataset consisting of a large corpus of in-the-wild videos with diverse scenes, camera movements and dense 3D annotations such as per-frame camera poses, depth, and motion instructions. Specifically, we collect more than 21,000 hours of raw video, and process

them into 2.7 million clips through a hierarchical filtering pipeline, totaling 7,089 hours of dynamic content. A subsequent annotation pipeline enriches these clips with detailed spatial and semantic information, including camera poses, depth maps, dynamic masks, structured captions, and serialized motion instructions. Analysis of SpatialVID’s data statistics reveals a richness and diversity that directly foster improved model generalization and performance, establishing it as a key asset for the video and 3D vision research community. Through extensive validation experiments, we demonstrate SpatialVID’s effectiveness across tasks such as controllable video generation, world simulation and geometric reconstruction, providing a strong foundation for spatial intelligence research.

1. Introduction

Perceiving, reasoning about, and interacting with the 3D world are fundamental components of artificial general intelligence. Recent advances in intrinsic 3D modeling have enabled the generation of spatially consistent and navigable environments directly from text or image prompts, bridging reconstruction and world simulation [5]. These models embody the dual objectives of understanding the current physical world and imagining plausible future ones.

The field of 3D scene understanding has evolved from optimization-based methods to scalable, data-driven representations of geometry and motion. Classical approaches such as Structure-from-Motion (SfM) [45] and neural Multi-View Stereo (MVS) [67] laid the foundation for geometric reasoning. Subsequently, large-scale neural models have recently emerged: the LRM series [18, 62, 75] learns to reconstruct high-quality 3D objects from single images or text prompts; DUS3R series [9, 58] achieve robust multi-view matching; VGGT [55] directly predicts key 3D attributes such as camera poses and point clouds in a feed-forward manner. Collectively, these models exemplify a shift toward scalable, data-driven reconstruction and synthesis with reduced reliance on explicit geometry. Despite these advancements, building large-scale 3D datasets remains challenging due to costly data acquisition and the reliance on accurate annotation pipelines [15, 43, 68]. In contrast, videos are abundant and naturally encode spatial, temporal, and semantic cues, offering a scalable foundation for 3D learning at scale. Leveraging such data presents a promising path toward high-fidelity reconstruction and dynamic world simulation.

Beyond reconstruction, video generation has emerged as a key capability for world modeling, serving as a simulator to represent and predict physical dynamics. Recent models including UNet-based diffusion methods like Stable Video Diffusion (SVD) [7], DiT-based architectures such as Sora [38], HunyuanVideo [25], and CogVideoX [66], as well as autoregressive approaches [6] enable high-fidelity video synthesis. To achieve controllable and physically grounded generation, recent efforts extend to object motion [69], camera trajectory control [17, 61], and 3D signal integration [72]. These capabilities represent crucial steps toward physically grounded video simulation and align with recent world models such as Cosmos [1], HunyuanWorld [52], and Genie3 [5]. Despite this progress, current datasets still lack detailed fine-grained semantic and spatial metadata, limiting their capacity to support physically grounded video synthesis.

Current data falls into two disjoint categories. Large-scale video datasets provide rich semantics but lack explicit 3D information [11, 37], offering no geometric ground truth and forcing models to learn spatial relations implicitly from pixels. Conversely, spatial datasets such as CO3D [42], RealEstate10K [82], and Tartanair [59] provide accurate geometry and camera parameters but remain small, object-

centric, or synthetic. This division hampers progress toward spatiotemporally coherent world simulators and underscores the need for a dataset that bridges *scene reconstruction* and *world simulation*, closing the gap between semantic diversity without geometry and geometric precision without semantics. To bridge the gap between dynamic videos and spatial understanding, we introduce **SpatialVID** (Fig. 1), a large-scale multimodal dataset that connects raw pixels to the physical world. Starting from over 21,000 hours of internet video manually screened for diversity and motion richness, we apply a hierarchical filtering pipeline to obtain 7,089 hours of high-quality 720P clips with reliable camera motion. From this corpus, we derive **SpatialVID-HQ**, a 1,111-hour balanced subset optimized for robust training and evaluation. Through extensive experiments, we demonstrate that SpatialVID advances tasks such as controllable video generation, world simulation and geometric reconstruction, providing a strong foundation for spatial intelligence research.

To our knowledge, SpatialVID is the largest dataset of dynamic videos with explicit geometric annotations and makes three primary contributions:

- **Manually Screened Videos with Camera Motions:** SpatialVID is built from 21,000+ hours of internet videos manually screened for rich scene motion. This motion-first curation and processing yield diverse, high-quality clips for training spatially aware models.
- **Comprehensive Geometric Annotations:** Each clip includes camera poses and depth maps generated via an adjusted pipeline [30], providing explicit 3D grounding and motion dynamics absent in prior video datasets.
- **Spatially-Aware Captions and Motion Instructions:** Structured captions describe scene content, camera motion, and semantic attributes (e.g., weather, lighting, time), while motion instructions derived from trajectories offer precise supervision for navigation and control tasks.

2. Related Work

Scene Reconstruction Traditionally, scene reconstruction has followed two main trajectories: Simultaneous Localization and Mapping (SLAM) and Structure-from-Motion (SfM). Classical systems such as ORB-SLAM [36] and COLMAP [45] achieve accurate geometry estimation and real-time tracking but depend heavily on handcrafted features, limiting robustness under challenging conditions. To overcome these constraints, learnable Multi-View Stereo (MVS) methods have emerged, with MVSNet [67] introducing deep cost-volume reasoning and Transformer-based models such as DUS3R [58], MAST3R [27], and their successors [9, 34, 64] achieving robust feed-forward multi-view matching. Recent frameworks like VGGT [55] further integrate these advances into end-to-end 3D reconstruction pipelines. Extending this trend to dynamic environments,

Table 1. **Comparisons with previous datasets with spatial information.** SpatialVID is a *million-level, dynamic and open-scenario* high-quality video dataset with rich annotated geometric and semantic information. Syn. denotes synthetic data; Sta. and Dyn. indicate static and dynamic scenes. In *Geometry Info.* column, C. denotes camera, D. denotes depth or point cloud.

Dataset	Domain	Real/Syn.	Dyn./Sta.	Geometry Info.	Caption	# Video Clips	# Frames
BlendedMVS [68]	Open	Syn.	Sta.	C. D.	Label	113 (Scenes)	17K
Multi-Cam Video [4]	Open	Syn.	Dyn.	C.	Label	136K	~11.02M
PointOdyssey [79]	Walk	Syn.	Dyn.	C. D.	N/A	159	200K
Camerabench [32]	Open	Real&Syn.	Dyn.	N/A	Label, Short	3,381	-
ScanNet [14]	Indoor	Real	Sta.	C. D.	N/A	1500 (Scenes)	2.50M
MVImgNet [73]	Object-Centric	Real	Sta.	C.	Label	219,188	6.50M
CO3Dv2 [42]	Object-Centric	Real	Sta.	C.	Label	19K	1.50M
DL3DV [33]	Open	Real	Sta.	N/A	Label	10,510	512M
WebVi3D [35]	Open	Real	Sta.	N/A	-	15.99M	320M
Dynpose100k [44]	Open	Real	Dyn.	C.	Short	100,131	6.81M
CamVid-30K [77]	Open	Real	Dyn.	C.	N/A	30K	-
Stereo4d [22]	Fisheye	Real	Dyn.	C. D.	Short	110K	10M
RealEstate10K [82]	Indoor	Real	Sta.	C.	N/A	~80K	~10M
Waymo [49]	Drive	Real	Dyn.	C.	N/A	1150	230K
Map-free [3]	Object-Centric	Real	Sta.	C.	N/A	655 (Scenes)	~560K
Princeton365 [24]	open	Real	Dyn.	C. D.	N/A	365	~1.19M
SpatialVID	Open	Real	Dyn.	C. D.	Structured Caption	2.71M	127.60M
SpatialVID-HQ	Open	Real	Dyn.	C. D.	Structured Caption	0.37M	20.63M

recent DUST3R variants [12, 57, 74] incorporate motion awareness extend the capabilities of DUST3R to incorporate dynamic elements, while dense approaches including CasualSAM [76] and MegaSAM [30] leverage optical flow or SLAM backbones [53] for robust tracking. Given its demonstrated robustness in unconstrained, in-the-wild videos, we utilize an enhanced version of MegaSAM in our work to generate the initial geometric annotations for our dataset.

World Simulator The concept of a world simulator lies at the core of spatial intelligence, encompassing the ability to perceive, simulate, and interact with dynamic environments. Recent progress in video generation has made this increasingly feasible. Early progress was driven by UNet-based video diffusion models such as Stable Video Diffusion (SVD) [7], followed by DiT-based architectures [25, 38, 66], which significantly advance fidelity, scalability, and temporal consistency. In parallel, autoregressive approaches [6, 70] remain competitive for generating high-quality, long-form videos. Achieving effective world simulation further requires controllability over 3D structure and motion. Models such as DragNUWA [69], CameraCtrl [17], and MotionCtrl [61] enable explicit manipulation of objects and camera trajectories, while GameFactory [71] introduces action-level control for interactive synthesis. Incorporating 3D data further enhances spatial coherence, as demonstrated by ViewCrafter [72], which integrates point clouds into video generation. These controlled and geometry-aware paradigms contribute to the development of world models such as Cosmos Predictor [1], HunyuanWorld [52], and Genie3 [5], aiming to simulate spatiotemporal dynamics and support interactive exploration within complex virtual environments.

Datasets with Spatial Annotations High-quality spatial datasets are crucial for advancing world reconstruction and exploration, ideally combining 3D geometry, dynamics, and semantic richness. Existing efforts fall into three main categories. Synthetic datasets such as Multi-Cam Video [4], virtualKITTI [8], and BlendedMVS [68] offer precise geometry information but demand heavy engineering, limiting scalability. Real-world datasets like CO3DV2 [42] and RealEstate10K [82] rely on SfM or SLAM-based annotation for efficiency, often yield sparse trajectories and struggle under dynamic motion. Video-mined datasets including CamVid-30K [77] and DynPose100K [44] provide large-scale semantic or motion cues but often lack fine-grained geometry or diversity. Recent datasets including CameraBench [32], VLM4D [81], and the concurrent Sekai [31] improve geometric-semantic integration but remain limited in semantic richness, motion coverage, or scale. To address these limitations, we introduce SpatialVID, a large-scale real-world dataset of diverse dynamic scenes with detailed geometric and semantic annotations. As shown in Tab. 1, SpatialVID outperforms prior datasets in scale and annotation quality, providing a rich foundation for spatially grounded representation learning and world simulation research.

3. SpatialVID Curation

As illustrated in Fig. 2, the SpatialVID curation pipeline comprises three main stages: filtering, annotation, and sampling. Sec. 3.1 covers video collection, format unification, and clip segmentation; Sec. 3.2 introduces multi-dimensional filtering based on four key metrics to retain diverse, motion-rich clips; Sec. 3.3 describes geometric annotation via camera

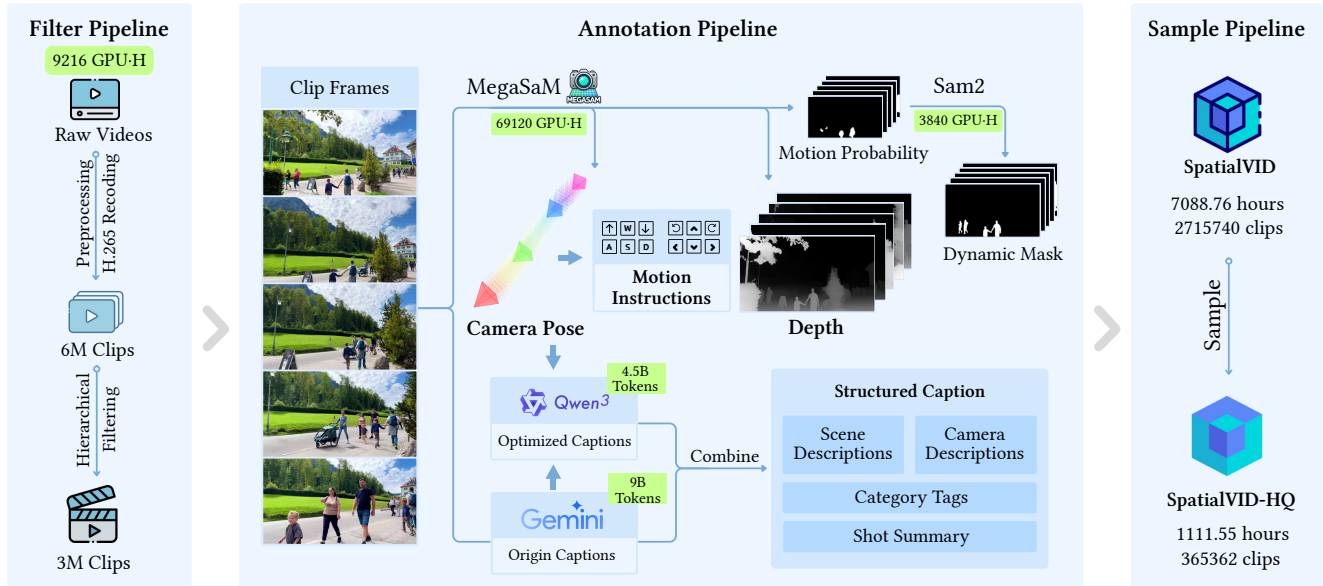


Figure 2. **Overview of the curation pipeline.** The pipeline comprises three stages: filtering, annotation, and sampling. We start from manually collected web videos with notable camera motion. In the **filtering stage**, raw videos are hierarchically preprocessed and filtered. The **annotation stage** adds geometric and semantic labels and derives motion instructions from camera poses. The **sampling stage** then balances clips by motion and category to form a high-quality subset (SpatialVID-HQ) with well-distributed classes for downstream tasks.

poses and depth maps; Sec. 3.4 details motion instruction generation; and Sec. 3.5 outlines structured captions integrating scene, motion, and semantic attributes.

3.1. Data Collection and Preprocessing

Source Data. While large-scale video datasets such as Panda70M [11] and MiraData [23] offer valuable benchmarks, they remain inadequate for our needs due to limited viewpoints and motion diversity. Processing the Panda70M validation split through our pipeline retained only about 10% of clips that met our quality standards, yielding insufficient data for large-scale reconstruction (Sec. 4.2).

To obtain richer and more varied data, we turned to YouTube, leveraging its vast and heterogeneous collection of high-resolution videos. We queried motion-related keywords (*walk*, *tour*, *drone*, etc.) to capture videos with smooth and diverse camera trajectories. Candidate videos were then manually screened for compatibility with the MegaSaM reconstruction pipeline. We excluded broken videos and videos with titles containing inappropriate terms (e.g., "Panoramic camera"). Footage with heavy occlusion or intrusive overlays (e.g., logos, subtitles) was also discarded.

This process yielded a curated corpus with stable motion, rich parallax, and detailed textures, ideal for 3D reconstruction. In total, we collected 33,443 YouTube videos (21,789 hours), covering a broad range of motion types, camera trajectories, and scene categories. Refer to Supplementary Materials for additional details about video statistics.

Data Preprocessing. We segment the collected long-form videos into 3–15 s clips using a modified PySceneDetect [10].

To better handle aesthetic transitions such as fades, we adjust sensitivity thresholds and adopt an interval-based multi-frame comparison strategy, significantly improving segmentation accuracy and efficiency. Given the variability in encoding formats and resolutions, all clips are then standardized to H.265-encoded MP4 at 1280×720 to ensure consistency and compatibility across the pipeline. After preprocessing, this yields over 7 million distinct video clips.

3.2. Video Quality Filtering

We filter all candidate videos using four key metrics: aesthetic quality, motion intensity, text interference, and luminance. This stage ensures that only clips with rich motion and clear visuals are retained, improving the reliability of downstream camera pose estimation. Given the large scale of our collection, such filtering is crucial for maintaining dataset quality and suitability for training and evaluation.

Specifically, we adopt a CLIP+MLP aesthetic predictor [47] to remove visually unappealing clips. Luminance filtering discards overexposed or underexposed samples to ensure consistent brightness. PaddleOCR [13] is used to detect and eliminate clips with excessive text based on the text-area ratio. Finally, motion filtering leverages lightweight VMAF metric [80] to retain videos with sufficient motion diversity for stable reconstruction. Representative filtering examples are provided in Supplementary Materials.

3.3. Geometry Information Annotation

We employ MegaSaM [30] as our primary camera estimator, chosen for its strong balance between accuracy and efficiency

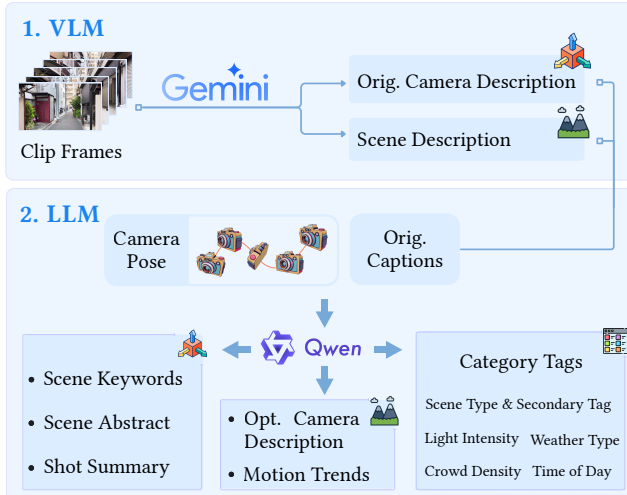


Figure 3. **Structured caption generation.** A VLM produces initial motion and scene descriptions, which the LLM refines using camera poses to yield structured captions.

compared to existing methods [46, 53, 55, 64, 74]. Comparisons of several methods are presented in Supplementary Materials. Our annotation pipeline is poised to improve by integrating future estimators with enhanced performance (e.g., ViPE [20]).

While effective, MegaSaM faces challenges under extreme conditions, such as dominant moving objects, collinear motion, or reliance on external monocular depth. To address these issues, we replace its original depth module with UniDepth v2 [39] and Depth Anything v2 [65], significantly improving depth accuracy and robustness. Furthermore, we first obtain candidate regions via adaptive thresholding and contour detection, then sample anchor points from them and use these as SAM2 [41] prompts to extract dynamic masks. From these refined masks, we compute *dynamic ratio* that quantifies the proportion of dynamic regions per frame.

To ensure physically plausible trajectories, we employ an acceleration-based detector to identify abrupt, non-physical motion fluctuations. Additionally, we introduce three metrics for quantitative camera motion analysis: (1) *MoveDist*, measuring total trajectory length; (2) *RotAngle*, capturing cumulative camera rotation; and (3) *TrajTurns*, estimating the number of significant directional changes.

3.4. Motion Instruction Decomposition

Given the importance of motion instructions for controllable and semantically grounded learning in models such as Hunyuan-GameCraft [29], our dataset explicitly incorporates them to enable interpretable motion understanding. We derive these instructions from estimated camera pose sequences, where relative translations and rotations between consecutive frames capture the camera’s motion dynamics. To enhance robustness, temporal smoothing filters are ap-

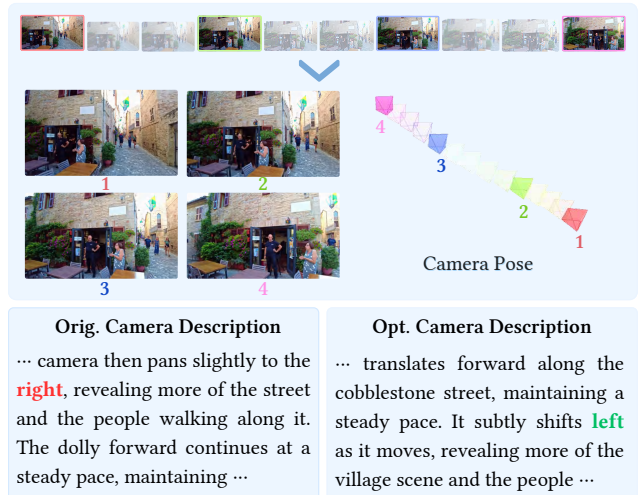


Figure 4. **Effect of spatial enhancement.** After applying spatial enhancement, the LLM corrected the incorrect direction (right) output by the VLM to left.

plied to suppress jitter and noise prior to instruction extraction. Perceptible motion segments are then identified through magnitude-based thresholding, generating instructions only when pose variations exceed predefined limits to avoid trivial movements. Finally, motion signals are mapped to a controlled vocabulary of cinematographic terms [32], such as *dolly in* (forward translation), *pan left* (horizontal rotation), and *truck right* (lateral translation). Visualized annotation results are provided in Supplementary Materials. This standardized decomposition ensures clarity, consistency, and semantic usability for downstream training.

3.5. Semantic Information Annotation

Multimodal models have made remarkable strides in bridging vision and language, employing diverse strategies for video caption generation. Early efforts such as VATEX [60] rely on manual annotation to ensure linguistic precision but lack scalability. More recent datasets [11, 37, 50] leverage multimodal large language models (MLLMs) for automatic caption generation, striking a balance between efficiency and semantic relevance. Others adopt structured or multi-stage pipelines [23, 56] to improve vision–text alignment, while OpenHumanVid [28] enhances caption reliability through LLM-based voting and reformatting. Despite these advances, vision–language models (VLMs) such as Gemini [51] remain limited in spatial reasoning, often overlooking geometric and camera-related details (Fig. 4). Recent works like CameraBench [32], VLM4D [81], and 3D LLM-Mem [19] highlight these shortcomings and explore early attempts to integrate depth and pose awareness.

Building upon these insights, we propose a structured caption generation framework that unifies VLM and LLM capabilities while explicitly incorporating camera poses (Fig. 3),

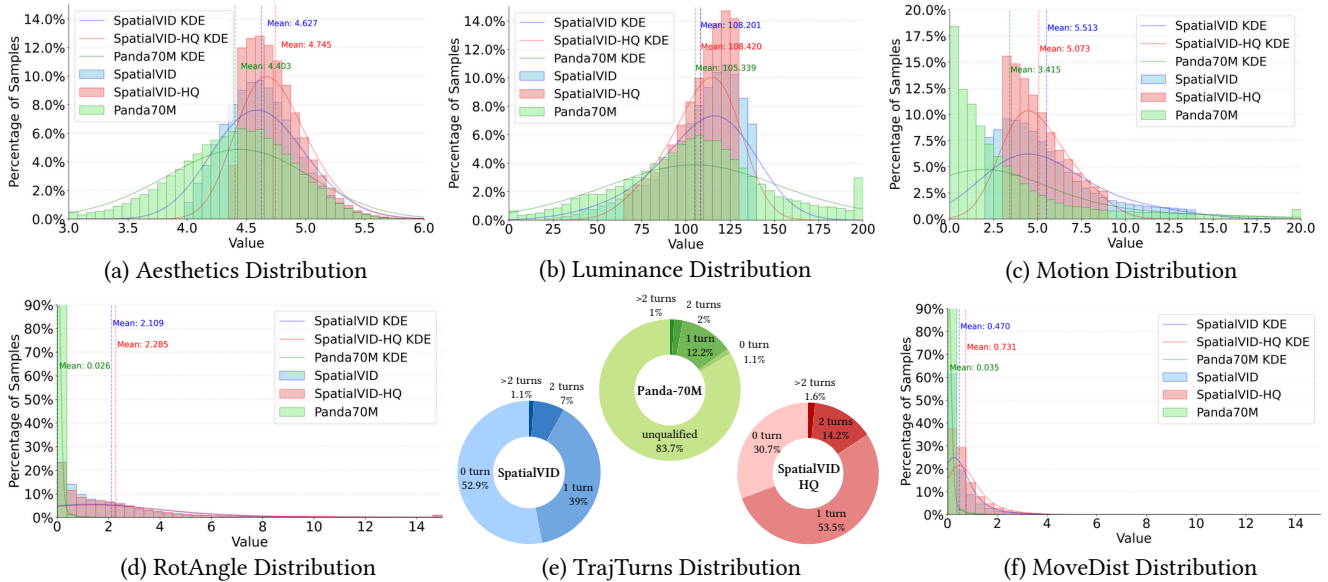


Figure 5. **Dataset quality comparison.** Comparison of SpatialVID, its balanced subset (SpatialVID-HQ), and the Panda70M-test set processed with the same pipeline. Histograms and KDE curves reveal distribution patterns across quality metrics, showing that SpatialVID-HQ achieves consistently superior quality, validating our manual collection, filtering, and sampling process.

enabling captions that are both semantically expressive and spatially grounded. Our pipeline operates in two stages: (1) *visual parsing*, where Gemini-2.0-Flash analyzes sampled frames to produce initial scene and motion descriptions; and (2) *language refinement*, where Qwen3-30B-A3B [63] refines these outputs using camera pose priors to correct motion directions and ensure spatial coherence. The refined captions integrate scene semantics, camera motion, and multi-level attributes (e.g., scene type, lighting, weather), forming a hierarchical textual representation that captures spatial, temporal, and cinematic structure. Further implementation details are provided in Supplementary Materials.

4. Dataset Analysis

4.1. Data Sampling

We aim to curate clips that maximize both quality and diversity. To this end, we first tighten thresholds across core quality metrics to elevate visual standards, and then balance semantic tags and trajectory statistics to ensure diversity. The resulting collection, SpatialVID-HQ, comprises over one thousand hours of high-quality spatial videos.

4.2. Comparison with Panda-70M

Panda-70M is a large-scale video dataset designed to support research on vision-language and video understanding. However, it exhibits several quality limitations: many clips are static, contain flickering artifacts, and include captions that lack motion descriptions. To demonstrate the advantages of our dataset, we perform a systematic comparison between SpatialVID and Panda-70M, as illustrated in Fig. 5.

Across key video-quality metrics including Aesthetics (Fig. 5a), Luminance (Fig. 5b), and Motion (Fig. 5c), both SpatialVID and its high-quality subset SpatialVID-HQ show more compact distributions, indicating greater consistency and higher average quality. Regarding camera motion statistics, Panda-70M is dominated by static viewpoints, as seen in the distributions of camera rotation (Fig. 5d) and translation distance (Fig. 5f). In contrast, SpatialVID achieves a balanced and realistic distribution of camera movements. Finally, Fig. 5e shows the distribution of trajectory turns (Arc Num): over 80% of Panda-70M videos cannot be reconstructed by MegaSaM due to insufficient motion, whereas SpatialVID-HQ deliberately increases the proportion of clips with curved or turning trajectories, providing a richer and more diverse motion profile.

5. SpatialVID Validation Tasks

In this section, we primarily evaluate the effectiveness of the SpatialVID dataset on camera-controlled video generation, which serves as our main task to assess spatially consistent visual synthesis. In addition, we conduct large-scale spatial reconstruction and pose estimation experiments as complementary validations, providing further evidence of the dataset’s quality and geometric fidelity.

5.1. Camera-Controlled Video Generation

Baseline. We build upon the camera-control injection mechanism introduced in ReCamMaster [4] (excluding intrinsic parameters), adopting the Wan2.2 architecture [54] as the base model and T5 [40] as the text encoder. For each frame,

Table 2. Quantitative comparison of camera-controlled video generation performance across different training datasets on Sekai-Real [31], RealEstate10K[82], and SpatialVID benchmarks.

Benchmark	Training Data	Camera Accuracy			Visual Quality		VBench				
		TransErr↓	RotErr↓	CamMC↓	CLIP-T↑	CLIP-F↑	Subject Consistency	Background Consistency	Motion Smoothness	Aesthetic Quality	Imaging Quality
RE10K	RE10K	7.46	1.15	7.91	30.38	99.53	96.45	94.52	99.05	55.99	72.71
	Sekai-Real	8.50	1.86	9.35	30.51	99.20	97.09	94.21	98.57	52.17	72.02
	<i>SpatialVID-HQ</i>	7.42	0.99	7.72	30.54	99.59	98.04	95.41	98.77	56.26	75.68
Sekai	RE10K	8.17	1.51	8.78	34.97	99.35	96.25	93.24	99.12	54.91	71.27
	Sekai-Real	6.49	1.47	7.12	33.98	98.57	93.25	91.24	98.06	52.53	72.32
	<i>SpatialVID-HQ</i>	6.04	1.43	6.70	35.19	99.28	96.39	93.49	98.88	54.14	73.13
SpatialVID	RE10K	5.16	4.07	8.59	30.22	99.02	94.31	92.70	98.68	55.00	66.23
	Sekai-Real	5.63	4.70	9.39	30.25	98.13	91.63	91.93	97.97	52.90	66.14
	<i>SpatialVID-HQ</i>	4.33	3.81	7.57	30.26	98.69	94.89	93.23	98.18	55.11	70.38

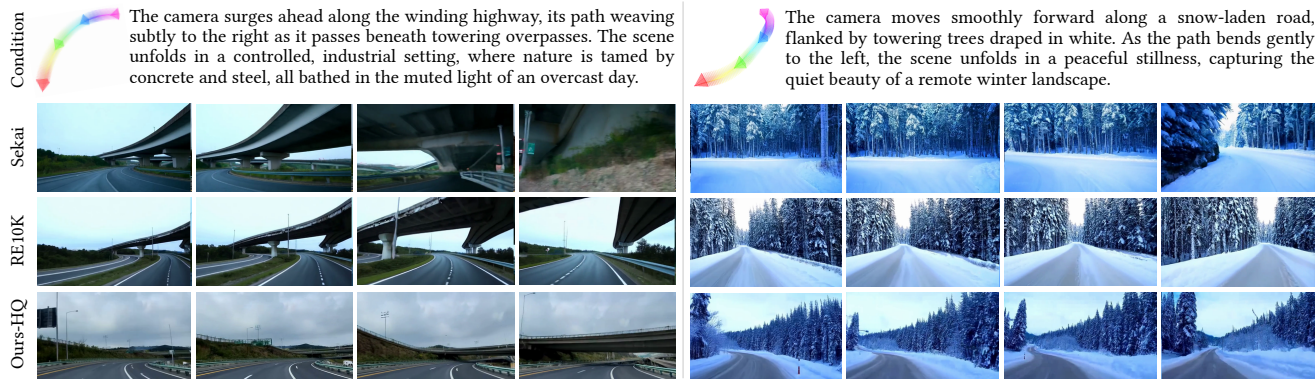


Figure 6. **Different training datasets performance on SpatialVID.** Under identical training settings, models trained on our dataset produce videos with more consistent appearance and significantly improved camera controllability.

camera extrinsics are processed by a learnable encoder E_c that projects them into the video token dimension. The encoded features are then fused with visual tokens and injected into each transformer block, enabling precise, frame-level camera control. We train models on Sekai-Real [31], RealEstate10K, and our SpatialVID-HQ subset under identical training configurations. Each model is fine-tuned on 32 H20 GPUs for 2 days and detailed training setup is provided in Supplementary Material.

Metrics. Following prior works [17, 78], we evaluate camera controllability using **TransErr**, **RotErr**, and **CamMC**, computed on poses estimated by MegaSaM [30]. For a fair and comprehensive comparison, all methods are evaluated on 100 randomly sampled sequences from the RealEstate10K test set [82], 300 sequences from the Sekai-Real test subset [31], and 500 unseen sequences from the SpatialVID dataset. These samples cover diverse subjects and a wide range of camera trajectories. Reported results are averaged across all sequences. Following ReCamMaster [4], we additionally report frame–text similarity (**CLIP-T**) and inter-frame temporal consistency (**CLIP-F**) [26], together with results on the widely used **VBench** metrics [21].

Results and Analysis. Quantitative results for camera-controlled video generation in Tab. 2 compare models

trained on different datasets across different benchmarks, all evaluated with camera pose and text as inputs. The analysis reveals that the model trained on *SpatialVID-HQ* consistently achieves the highest accuracy in camera control across all three benchmarks, demonstrating the high quality of the camera pose annotations and the strong generalization capability of our dataset. Additionally, models trained on *SpatialVID-HQ* attain the highest CLIP-T, reflecting enhanced visual fidelity and text-video alignment. It further shows stable improvements across all VBench metrics, particularly in Imaging Quality. Qualitative comparisons in Fig. 6 show that videos generated from models trained on *SpatialVID-HQ* exhibit greater realism and temporal consistency, benefiting from the dataset’s diverse trajectories, high-quality videos, and consistent text annotations.

5.2. Novel View Synthesis

Baseline. Recent large reconstruction models for novel view synthesis, such as GS-LRM [75] and Long-LRM [83], have demonstrated strong scene-level 3D reconstruction capabilities. We adopt GS-LRM as our baseline framework, which combines a Transformer-based architecture with 3D Gaussian rendering for high-fidelity scene recovery. For fairness, GS-LRM is trained separately on RealEstate10K

Table 3. Comparison of Original and Fine-tuned Models for Camera Pose Estimation on Sintel [2], TUM-dynamics [48], and Dycheck [16].

Method	Sintel			TUM-dynamics			Dycheck		
	ATE↓	RPE trans↓	RPE rot↓	ATE↓	RPE trans↓	RPE rot↓	ATE↓	RPE trans↓	RPE rot↓
CUT3R	0.210	0.070	0.637	0.049	0.015	0.449	0.020	0.011	1.275
CUT3R (Fine-tuned)	0.210	0.069	0.619	0.040	0.013	0.395	0.019	0.011	1.184
VGGT	0.134	0.079	0.501	0.015	0.013	0.352	0.005	0.008	1.087
VGGT (Fine-tuned)	0.148	0.075	0.462	0.013	0.011	0.312	0.005	0.009	1.090

Table 4. Comparison of GS-LRM across different training datasets on DL3DV [33] and our SpatialVID.

Training Data	DL3DV			SpatialVID		
	PSNR ↑	SSIM ↑	LPIPS ↓	PSNR ↑	SSIM ↑	LPIPS ↓
RE10K	27.01	0.889	0.132	24.13	0.774	0.222
SpatialVID	27.80	0.892	0.116	24.97	0.790	0.203

and a SpatialVID-HQ subset under identical configurations and data volumes. The SpatialVID-HQ subset is curated to match the number of clips in RealEstate10K, prioritizing static scenes for consistency. Each model is finetuned on 8 A6000 GPUs for 3 days and detailed training setup is provided in Supplementary Materials.

Metrics. We follow GS-LRM [75] and evaluate novel-view synthesis using PSNR, SSIM, and LPIPS. Experiments are conducted on 500 DL3DV [33] and 500 unseen SpatialVID sequences, with 2 reference and 4 target views per sequence, rendered at 360×640 for a fair comparison.

Results and Analysis. As shown in Tab. 4, the model trained on the SpatialVID subset consistently outperforms RealEstate10K across all the metrics. These results highlight the strong generalization capability of SpatialVID, with superior performance even on the predominantly outdoor DL3DV scenes. This suggests that the diversity and quality of SpatialVID data lead to more robust scene understanding and higher-quality novel view synthesis. Further results are provided in Supplementary Materials.

5.3. Geometric Prediction

Baselines. For camera pose estimation task, we adopt CUT3R [57] and VGGT [55] as representative baselines, both demonstrating strong performance in geometric and structural reconstruction. Each model is initialized from its official pre-trained weights and fine-tuned under comparable settings. CUT3R is further fine-tuned on SpatialVID to assess pose consistency improvements, while VGGT is trained on its original data both with and without SpatialVID-HQ for fair comparison. Each model is fine-tuned on 8 H20 GPUs for 2 days and detailed training setup is provided in Supplementary Materials.

Metrics. For geometric prediction we focus on camera-pose estimation in dynamic scenes. We evaluate models on three diverse benchmarks including Sintel [2], TUM-

dynamics [48], and Dycheck [16], all containing non-rigid and dynamic objects to ensure comprehensive coverage of different data types and scene characteristics. Following previous works [57, 74], we report ATE, RPE-rot and RPE-trans computed over estimated camera trajectories.

Results and Analysis. Both CUT3R and VGGT are trained on multiple 3D-annotated datasets and already achieve strong results, though most training data are synthetic. SpatialVID, covering diverse real-world scenes, complements these sources and improves generalization to realistic conditions. As shown in Tab. 3, fine-tuning on SpatialVID yields notable gains for both models on the TUM-dynamics benchmark. On the synthetic Sintel benchmark, both models show improvements, except for a slight ATE regression for VGGT. The Dycheck benchmark, with high dynamics and complex camera trajectories from handheld jitter, remains challenging. After fine-tuning, CUT3R’s performance is marginally improved, while VGGT, near its ceiling, exhibits only minor fluctuations, reflecting its strong pre-trained capability.

6. Discussion and Conclusion

Limitations. Our annotation pipeline inherits failure modes from MegaSaM and can degrade under extreme scenarios (e.g., object-dominated frames, varying focal lengths, and severe radial distortion), constraining its broader application. Additionally, the predicted camera poses exhibit non-metric properties in specific scenarios, and masks derived from motion probabilities yield suboptimal performance in complex scenes. We expect that the development of advanced video pose estimator (e.g., ViPE [20]) would mitigate these issues in the future.

Conclusion. We introduce SpatialVID, a large-scale video dataset spanning diverse real-world scenes, with tightly aligned semantic and geometric annotations. Our procedural pipeline distills in-the-wild videos into clips annotated with camera motion, depth, and structured, motion-aware scene descriptions. By unifying explicit 3D motion control with rich textual semantics, SpatialVID provides strong 3D inductive biases for physically grounded video generation, dynamic scene synthesis, and spatial intelligence. Extensive experiments demonstrate its effectiveness across multiple tasks, establishing a robust foundation for future research.

References

- [1] Niket Agarwal, Arslan Ali, Maciej Bala, Yogesh Balaji, Erik Barker, Tiffany Cai, Prithvijit Chattopadhyay, Yongxin Chen, Yin Cui, Yifan Ding, et al. Cosmos world foundation model platform for physical ai. *arXiv preprint arXiv:2501.03575*, 2025. 2, 3
- [2] Sarah Alnegheimish, Dongyu Liu, Carles Sala, Laure Berti-Equille, and Kalyan Veeramachaneni. Sintel: A machine learning framework to extract insights from signals. In *Proceedings of the 2022 International Conference on Management of Data*, pages 1855–1865, 2022. 8
- [3] Eduardo Arnold, Jamie Wynn, Sara Vicente, Guillermo Garcia-Hernando, Áron Monzpart, Victor Adrian Prisacariu, Daniyar Turmukhambetov, and Eric Brachmann. Map-free visual relocalization: Metric pose relative to a single image. In *ECCV*, 2022. 3
- [4] Jianhong Bai, Menghan Xia, Xiao Fu, Xintao Wang, Lianrui Mu, Jinwen Cao, Zuozhu Liu, Haoji Hu, Xiang Bai, Pengfei Wan, et al. Recammaster: Camera-controlled generative rendering from a single video. *arXiv preprint arXiv:2503.11647*, 2025. 3, 6, 7, 19
- [5] Philip J. Ball, Jakob Bauer, Frank Belletti, Bethanie Brownfield, Ariel Ephrat, Shlomi Fruchter, Agrim Gupta, Kristian Holsheimer, Aleksander Holynski, Jiri Hron, and et al. Genie 3: A new frontier for world models. 2025. 2, 3
- [6] Adrien Bardes, Quentin Garrido, Jean Ponce, Xinlei Chen, Michael Rabbat, Yann LeCun, Mahmoud Assran, and Nicolas Ballas. Revisiting feature prediction for learning visual representations from video. *arXiv preprint arXiv:2404.08471*, 2024. 2, 3
- [7] Andreas Blattmann, Tim Dockhorn, Sumith Kulal, Daniel Mendelevitch, Maciej Kilian, Dominik Lorenz, Yam Levi, Zion English, Vikram Voleti, Adam Letts, et al. Stable video diffusion: Scaling latent video diffusion models to large datasets. *arXiv preprint arXiv:2311.15127*, 2023. 2, 3
- [8] Johann Cabon, Naila Murray, and Martin Humenberger. Virtual kitti 2. *arXiv preprint arXiv:2001.10773*, 2020. 3
- [9] Johann Cabon, Lucas Stofl, Leonid Antsfeld, Gabriela Csurka, Boris Chidlovskii, Jerome Revaud, and Vincent Leroy. Must3r: Multi-view network for stereo 3d reconstruction. In *Proceedings of the Computer Vision and Pattern Recognition Conference*, pages 1050–1060, 2025. 2
- [10] Brandon Castellano. Pyscenedetect. 4
- [11] Tsai-Shien Chen, Aliaksandr Siarohin, Willi Menapace, Ekaterina Deyneka, Hsiang-wei Chao, Byung Eun Jeon, Yuwei Fang, Hsin-Ying Lee, Jian Ren, Ming-Hsuan Yang, et al. Panda-70m: Captioning 70m videos with multiple cross-modality teachers. *arXiv preprint arXiv:2402.19479*, 2024. 2, 4, 5
- [12] Xingyu Chen, Yue Chen, Yuliang Xiu, Andreas Geiger, and Anpei Chen. Easi3r: Estimating disentangled motion from dust3r without training. *arXiv preprint arXiv:2503.24391*, 2025. 3
- [13] Cheng Cui, Ting Sun, Manhui Lin, Tingquan Gao, Yubo Zhang, Jiakuan Liu, Xueqing Wang, Zelun Zhang, Changda Zhou, Hongen Liu, et al. Paddleocr 3.0 technical report. *arXiv preprint arXiv:2507.05595*, 2025. 4, 13
- [14] Angela Dai, Angel X Chang, Manolis Savva, Maciej Halber, Thomas Funkhouser, and Matthias Nießner. Scannet: Richly-annotated 3d reconstructions of indoor scenes. In *Proceedings of the IEEE conference on computer vision and pattern recognition*, pages 5828–5839, 2017. 3
- [15] Matt Deitke, Dustin Schwenk, Jordi Salvador, Luca Weihs, Oscar Michel, Eli VanderBilt, Ludwig Schmidt, Kiana Ehsani, Aniruddha Kembhavi, and Ali Farhadi. Objaverse: A universe of annotated 3d objects. In *Proceedings of the IEEE/CVF conference on computer vision and pattern recognition*, pages 13142–13153, 2023. 2
- [16] Hang Gao, Ruilong Li, Shubham Tulsiani, Bryan Russell, and Angjoo Kanazawa. Monocular dynamic view synthesis: A reality check. *Advances in Neural Information Processing Systems*, 35:33768–33780, 2022. 8
- [17] Hao He, Yinghao Xu, Yuwei Guo, Gordon Wetzstein, Bo Dai, Hongsheng Li, and Ceyuan Yang. Cameractrl: Enabling camera control for text-to-video generation. *arXiv preprint arXiv:2404.02101*, 2024. 2, 3, 7, 18
- [18] Yicong Hong, Kai Zhang, Jiuxiang Gu, Sai Bi, Yang Zhou, Difan Liu, Feng Liu, Kalyan Sunkavalli, Trung Bui, and Hao Tan. Lrm: Large reconstruction model for single image to 3d. *arXiv preprint arXiv:2311.04400*, 2023. 2
- [19] Wenbo Hu, Yining Hong, Yanjun Wang, Leison Gao, Zibu Wei, Xingcheng Yao, Nanyun Peng, Yonatan Bitton, Idan Szepes, and Kai-Wei Chang. 3dllm-mem: Long-term spatial-temporal memory for embodied 3d large language model. *arXiv preprint arXiv:2505.22657*, 2025. 5
- [20] Jiahui Huang, Qunjie Zhou, Hesam Rabeti, Aleksandr Korovko, Huan Ling, Xuanchi Ren, Tianchang Shen, Jun Gao, Dmitry Slepichev, Chen-Hsuan Lin, et al. Vipe: Video pose engine for 3d geometric perception. *arXiv preprint arXiv:2508.10934*, 2025. 5, 8
- [21] Ziqi Huang, Yanan He, Jiashuo Yu, Fan Zhang, Chenyang Si, Yuming Jiang, Yuanhan Zhang, Tianxing Wu, Qingyang Jin, Nattapol Chanpaisit, et al. Vbench: Comprehensive benchmark suite for video generative models. In *Proceedings of the IEEE/CVF Conference on Computer Vision and Pattern Recognition*, pages 21807–21818, 2024. 7
- [22] Linyi Jin, Richard Tucker, Zhengqi Li, David Fouhey, Noah Snavely, and Aleksander Holynski. Stereo4d: Learning how things move in 3d from internet stereo videos. *arXiv preprint arXiv:2412.09621*, 2024. 3
- [23] Xuan Ju, Yiming Gao, Zhaoyang Zhang, Ziyang Yuan, Xintao Wang, Ailing Zeng, Yu Xiong, Qiang Xu, and Ying Shan. Miradata: A large-scale video dataset with long durations and structured captions, 2024. 4, 5
- [24] Karhan Kayan, Stamatis Alexandropoulos, Rishabh Jain, Yiming Zuo, Erich Liang, and Jia Deng. Princeton365: A diverse dataset with accurate camera pose, 2025. 3
- [25] Weijie Kong, Qi Tian, Zijian Zhang, Rox Min, Zuozhuo Dai, Jin Zhou, Jiangfeng Xiong, Xin Li, Bo Wu, Jianwei Zhang, et al. Hunyuanvideo: A systematic framework for large video generative models. *arXiv preprint arXiv:2412.03603*, 2024. 2, 3
- [26] Zhengfei Kuang, Shengqu Cai, Hao He, Yinghao Xu, Hongsheng Li, Leonidas J Guibas, and Gordon Wetzstein. Collaborative video diffusion: Consistent multi-video generation with

- camera control. *Advances in Neural Information Processing Systems*, 37:16240–16271, 2024. 7
- [27] Vincent Leroy, Yann Cabon, and Jérôme Revaud. Grounding image matching in 3d with mast3r. In *European Conference on Computer Vision*, pages 71–91. Springer, 2024. 2
- [28] Hui Li, Mingwang Xu, Yun Zhan, Shan Mu, Jiaye Li, Kaihui Cheng, Yuxuan Chen, Tan Chen, Mao Ye, Jingdong Wang, et al. Openhumanvid: A large-scale high-quality dataset for enhancing human-centric video generation. In *Proceedings of the Computer Vision and Pattern Recognition Conference*, pages 7752–7762, 2025. 5
- [29] Jiaqi Li, Junshu Tang, Zhiyong Xu, Longhuang Wu, Yuan Zhou, Shuai Shao, Tianbao Yu, Zhiguo Cao, and Qinglin Lu. Hunyuan-gamecraft: High-dynamic interactive game video generation with hybrid history condition, 2025. 5
- [30] Zhengqi Li, Richard Tucker, Forrester Cole, Qianqian Wang, Linyi Jin, Vickie Ye, Angjoo Kanazawa, Aleksander Holynski, and Noah Snavely. Megasam: Accurate, fast and robust structure and motion from casual dynamic videos. In *arxiv*, 2024. 2, 3, 4, 7
- [31] Zhen Li, Chuanhao Li, Xiaofeng Mao, Shaoheng Lin, Ming Li, Shitian Zhao, Zhaopan Xu, Xinyue Li, Yukang Feng, Jianwen Sun, et al. Sekai: A video dataset towards world exploration. *arXiv preprint arXiv:2506.15675*, 2025. 3, 7, 18
- [32] Zhiqiu Lin, Siyuan Cen, Daniel Jiang, Jay Karhade, Hewei Wang, Chancharik Mitra, Tiffany Ling, Yuhan Huang, Sifan Liu, Mingyu Chen, et al. Towards understanding camera motions in any video. *arXiv preprint arXiv:2504.15376*, 2025. 3, 5
- [33] Lu Ling, Yichen Sheng, Zhi Tu, Wentian Zhao, Cheng Xin, Kun Wan, Lantao Yu, Qianyu Guo, Zixun Yu, Yawen Lu, et al. D13dv-10k: A large-scale scene dataset for deep learning-based 3d vision. In *Proceedings of the IEEE/CVF Conference on Computer Vision and Pattern Recognition*, pages 22160–22169, 2024. 3, 8
- [34] Jiahao Lu, Tianyu Huang, Peng Li, Zhiyang Dou, Cheng Lin, Zhiming Cui, Zhen Dong, Sai-Kit Yeung, Wenping Wang, and Yuan Liu. Align3r: Aligned monocular depth estimation for dynamic videos. In *Proceedings of the Computer Vision and Pattern Recognition Conference*, pages 22820–22830, 2025. 2
- [35] Baorui Ma, Huachen Gao, Haoge Deng, Zhengxiong Luo, Tiejun Huang, Lulu Tang, and Xinlong Wang. You see it, you got it: Learning 3d creation on pose-free videos at scale. In *Proceedings of the Computer Vision and Pattern Recognition Conference*, pages 2016–2029, 2025. 3
- [36] Raul Mur-Artal, Jose Maria Martinez Montiel, and Juan D Tardos. Orb-slam: A versatile and accurate monocular slam system. *IEEE transactions on robotics*, 31(5):1147–1163, 2015. 2
- [37] Kepan Nan, Rui Xie, Penghao Zhou, Tiehan Fan, Zhenheng Yang, Zhijie Chen, Xiang Li, Jian Yang, and Ying Tai. Openvid-1m: A large-scale high-quality dataset for text-to-video generation. *arXiv preprint arXiv:2407.02371*, 2024. 2, 5
- [38] OpenAI. Video generation models as world simulators, 2024. Accessed: 2024-02-15. 2, 3
- [39] Luigi Piccinelli, Christos Sakaridis, Yung-Hsu Yang, Mattia Segu, Siyuan Li, Wim Abbeloos, and Luc Van Gool. UniDepthV2: Universal monocular metric depth estimation made simpler, 2025. 5
- [40] Colin Raffel, Noam Shazeer, Adam Roberts, Katherine Lee, Sharan Narang, Michael Matena, Yanqi Zhou, Wei Li, and Peter J Liu. Exploring the limits of transfer learning with a unified text-to-text transformer. *Journal of machine learning research*, 21(140):1–67, 2020. 6
- [41] Nikhila Ravi, Valentin Gabeur, Yuan-Ting Hu, Ronghang Hu, Chaitanya Ryal, Tengyu Ma, Haitham Khedr, Roman Rädle, Chloe Rolland, Laura Gustafson, Eric Mintun, Junting Pan, Kalyan Vasudev Alwala, Nicolas Carion, Chao-Yuan Wu, Ross Girshick, Piotr Dollár, and Christoph Feichtenhofer. Sam 2: Segment anything in images and videos. *arXiv preprint arXiv:2408.00714*, 2024. 5
- [42] Jeremy Reizenstein, Roman Shapovalov, Philipp Henzler, Luca Sbordone, Patrick Labatut, and David Novotny. Common objects in 3d: Large-scale learning and evaluation of real-life 3d category reconstruction. In *Proceedings of the IEEE/CVF International Conference on Computer Vision*, pages 10901–10911, 2021. 2, 3
- [43] Mike Roberts, Jason Ramapuram, Anurag Ranjan, Atulit Kumar, Miguel Angel Bautista, Nathan Paczan, Russ Webb, and Joshua M Susskind. Hypersim: A photorealistic synthetic dataset for holistic indoor scene understanding. In *Proceedings of the IEEE/CVF international conference on computer vision*, pages 10912–10922, 2021. 2
- [44] Chris Rockwell, Joseph Tung, Tsung-Yi Lin, Ming-Yu Liu, David F Fouhey, and Chen-Hsuan Lin. Dynamic camera poses and where to find them. In *Proceedings of the Computer Vision and Pattern Recognition Conference*, pages 12444–12455, 2025. 3
- [45] Johannes L. Schonberger and Jan-Michael Frahm. Structure-from-motion revisited. In *Proceedings of the IEEE Conference on Computer Vision and Pattern Recognition (CVPR)*, 2016. 2
- [46] Johannes Lutz Schönberger and Jan-Michael Frahm. Structure-from-motion revisited. In *Conference on Computer Vision and Pattern Recognition (CVPR)*, 2016. 5, 13
- [47] Christoph Schuhmann, Romain Beaumont, Richard Vencu, Cade Gordon, Ross Wightman, Mehdi Cherti, Theo Coombes, Aarush Katta, Clayton Mullis, Mitchell Wortsman, et al. Laion-5b: An open large-scale dataset for training next generation image-text models. *Advances in neural information processing systems*, 35:25278–25294, 2022. 4, 13
- [48] Jürgen Sturm, Nikolas Engelhard, Felix Endres, Wolfram Burgard, and Daniel Cremers. A benchmark for the evaluation of rgb-d slam systems. In *2012 IEEE/RSJ international conference on intelligent robots and systems*, pages 573–580. IEEE, 2012. 8
- [49] Pei Sun, Henrik Kretzschmar, Xerxes Dotiwalla, Aurelien Chouard, Vijaysai Patnaik, Paul Tsui, James Guo, Yin Zhou, Yuning Chai, Benjamin Caine, et al. Scalability in perception for autonomous driving: Waymo open dataset. In *Proceedings of the IEEE/CVF conference on computer vision and pattern recognition*, pages 2446–2454, 2020. 3

- [50] Zhiyu Tan, Xiaomeng Yang, Luozheng Qin, and Hao Li. Vidgen-1m: A large-scale dataset for text-to-video generation. *arXiv preprint arXiv:2408.02629*, 2024. 5
- [51] Gemini Team, Rohan Anil, Sebastian Borgeaud, Jean-Baptiste Alayrac, Jiahui Yu, Radu Soricut, Johan Schalkwyk, Andrew M Dai, Anja Hauth, Katie Millican, et al. Gemini: a family of highly capable multimodal models. *arXiv preprint arXiv:2312.11805*, 2023. 5, 13
- [52] HunyuanWorld Team, Zhenwei Wang, Yuhao Liu, Junta Wu, Zixiao Gu, Haoyuan Wang, Xuhui Zuo, Tianyu Huang, Wenhuan Li, Sheng Zhang, et al. Hunyuanworld 1.0: Generating immersive, explorable, and interactive 3d worlds from words or pixels. *arXiv preprint arXiv:2507.21809*, 2025. 2, 3
- [53] Zachary Teed and Jia Deng. Droid-slam: Deep visual slam for monocular, stereo, and rgb-d cameras. *Advances in neural information processing systems*, 34:16558–16569, 2021. 3, 5, 13
- [54] Team Wan, Ang Wang, Baole Ai, Bin Wen, Chaojie Mao, Chen-Wei Xie, Di Chen, Feiwei Yu, Haiming Zhao, Jianxiao Yang, et al. Wan: Open and advanced large-scale video generative models. *arXiv preprint arXiv:2503.20314*, 2025. 6, 18
- [55] Jianyuan Wang, Minghao Chen, Nikita Karaev, Andrea Vedaldi, Christian Rupprecht, and David Novotny. Vggt: Visual geometry grounded transformer. In *Proceedings of the Computer Vision and Pattern Recognition Conference*, pages 5294–5306, 2025. 2, 5, 8, 13, 25
- [56] Qiheng Wang, Yukai Shi, Jiarong Ou, Rui Chen, Ke Lin, Jiahao Wang, Boyuan Jiang, Haotian Yang, Mingwu Zheng, Xin Tao, et al. Koala-36m: A large-scale video dataset improving consistency between fine-grained conditions and video content. In *Proceedings of the Computer Vision and Pattern Recognition Conference*, pages 8428–8437, 2025. 5
- [57] Qianqian Wang*, Yifei Zhang*, Aleksander Holynski, Alexei A. Efros, and Angjoo Kanazawa. Continuous 3d perception model with persistent state. In *CVPR*, 2025. 3, 8, 25
- [58] Shuzhe Wang, Vincent Leroy, Yohann Cabon, Boris Chidlovskii, and Jerome Revaud. Dust3r: Geometric 3d vision made easy. In *Proceedings of the IEEE/CVF Conference on Computer Vision and Pattern Recognition*, pages 20697–20709, 2024. 2
- [59] Wenshan Wang, DeLong Zhu, Xiangwei Wang, Yaoyu Hu, Yuheng Qiu, Chen Wang, Yafei Hu, Ashish Kapoor, and Sebastian Scherer. Tartanair: A dataset to push the limits of visual slam. In *2020 IEEE/RSJ International Conference on Intelligent Robots and Systems (IROS)*, pages 4909–4916. IEEE, 2020. 2
- [60] Xin Wang, Jiawei Wu, Junkun Chen, Lei Li, Yuan-Fang Wang, and William Yang Wang. Vatex: A large-scale, high-quality multilingual dataset for video-and-language research. In *Proceedings of the IEEE/CVF international conference on computer vision*, pages 4581–4591, 2019. 5
- [61] Zhouxia Wang, Ziyang Yuan, Xintao Wang, Yaowei Li, Tianshui Chen, Menghan Xia, Ping Luo, and Ying Shan. Motionctrl: A unified and flexible motion controller for video generation. In *ACM SIGGRAPH 2024 Conference Papers*, pages 1–11, 2024. 2, 3
- [62] Xinyue Wei, Kai Zhang, Sai Bi, Hao Tan, Fujun Luan, Valentin Deschaintre, Kalyan Sunkavalli, Hao Su, and Zexiang Xu. Meshlrn: Large reconstruction model for high-quality meshes. *arXiv preprint arXiv:2404.12385*, 2024. 2
- [63] An Yang, Anfeng Li, Baosong Yang, Beichen Zhang, Binyuan Hui, Bo Zheng, Bowen Yu, Chang Gao, Chengen Huang, Chenxu Lv, et al. Qwen3 technical report. *arXiv preprint arXiv:2505.09388*, 2025. 6, 13
- [64] Jianing Yang, Alexander Sax, Kevin J Liang, Mikael Henaff, Hao Tang, Ang Cao, Joyce Chai, Franziska Meier, and Matt Feiszli. Fast3r: Towards 3d reconstruction of 1000+ images in one forward pass. In *Proceedings of the Computer Vision and Pattern Recognition Conference*, pages 21924–21935, 2025. 2, 5, 13
- [65] Lihe Yang, Bingyi Kang, Zilong Huang, Zhen Zhao, Xiaogang Xu, Jiashi Feng, and Hengshuang Zhao. Depth anything v2. *arXiv:2406.09414*, 2024. 5
- [66] Zhuoyi Yang, Jiayan Teng, Wendi Zheng, Ming Ding, Shiyu Huang, Jiazheng Xu, Yuanming Yang, Wenyi Hong, Xiaohan Zhang, Guanyu Feng, et al. Cogvideox: Text-to-video diffusion models with an expert transformer. *arXiv preprint arXiv:2408.06072*, 2024. 2, 3
- [67] Yao Yao, Zixin Luo, Shiwei Li, Tian Fang, and Long Quan. Mvsnet: Depth inference for unstructured multi-view stereo. In *Proceedings of the European conference on computer vision (ECCV)*, pages 767–783, 2018. 2
- [68] Yao Yao, Zixin Luo, Shiwei Li, Jingyang Zhang, Yufan Ren, Lei Zhou, Tian Fang, and Long Quan. Blendedmvs: A large-scale dataset for generalized multi-view stereo networks. In *Proceedings of the IEEE/CVF conference on computer vision and pattern recognition*, pages 1790–1799, 2020. 2, 3
- [69] Shengming Yin, Chenfei Wu, Jian Liang, Jie Shi, Houqiang Li, Gong Ming, and Nan Duan. Dragnuwa: Fine-grained control in video generation by integrating text, image, and trajectory. *arXiv preprint arXiv:2308.08089*, 2023. 2, 3
- [70] Jiwen Yu, Jianhong Bai, Yiran Qin, Quande Liu, Xintao Wang, Pengfei Wan, Di Zhang, and Xihui Liu. Context as memory: Scene-consistent interactive long video generation with memory retrieval. *arXiv preprint arXiv:2506.03141*, 2025. 3
- [71] Jiwen Yu, Yiran Qin, Xintao Wang, Pengfei Wan, Di Zhang, and Xihui Liu. Gamefactory: Creating new games with generative interactive videos. *arXiv preprint arXiv:2501.08325*, 2025. 3
- [72] Wangbo Yu, Jinbo Xing, Li Yuan, Wenbo Hu, Xiaoyu Li, Zhipeng Huang, Xiangjun Gao, Tien-Tsin Wong, Ying Shan, and Yonghong Tian. Viewcrafter: Taming video diffusion models for high-fidelity novel view synthesis. *arXiv preprint arXiv:2409.02048*, 2024. 2, 3
- [73] Xianggang Yu, Mutian Xu, Yidan Zhang, Haolin Liu, Chongjie Ye, Yushuang Wu, Zizheng Yan, Tianyou Liang, Guanying Chen, Shuguang Cui, and Xiaoguang Han. Mvimnet: A large-scale dataset of multi-view images. In *CVPR*, 2023. 3
- [74] Junyi Zhang, Charles Herrmann, Junhwa Hur, Varun Jampani, Trevor Darrell, Forrester Cole, Deqing Sun, and Ming-Hsuan Yang. Monst3r: A simple approach for estimating geometry

- in the presence of motion. *arXiv preprint arxiv:2410.03825*, 2024. [3](#), [5](#), [8](#), [13](#)
- [75] Kai Zhang, Sai Bi, Hao Tan, Yuanbo Xiangli, Nanxuan Zhao, Kalyan Sunkavalli, and Zexiang Xu. Gs-lrm: Large reconstruction model for 3d gaussian splatting. In *European Conference on Computer Vision*, pages 1–19. Springer, 2024. [2](#), [7](#), [8](#), [25](#)
- [76] Zhoutong Zhang, Forrester Cole, Zhengqi Li, Michael Rubinstein, Noah Snavely, and William T Freeman. Structure and motion from casual videos. In *European Conference on Computer Vision*, pages 20–37. Springer, 2022. [3](#)
- [77] Yuyang Zhao, Chung-Ching Lin, Kevin Lin, Zhiwen Yan, Linjie Li, Zhengyuan Yang, Jianfeng Wang, Gim Hee Lee, and Lijuan Wang. Genxd: Generating any 3d and 4d scenes. *arXiv preprint arXiv:2411.02319*, 2024. [3](#)
- [78] Guangcong Zheng, Teng Li, Rui Jiang, Yehao Lu, Tao Wu, and Xi Li. Cami2v: Camera-controlled image-to-video diffusion model. *arXiv preprint arXiv:2410.15957*, 2024. [7](#)
- [79] Yang Zheng, Adam W. Harley, Bokui Shen, Gordon Wetstein, and Leonidas J. Guibas. Pointodyssey: A large-scale synthetic dataset for long-term point tracking. In *ICCV*, 2023. [3](#)
- [80] Li Zhi, Aaron Anne, Katsavounidis Ioannis, Moorthy Anush, and Manohara Megha. Toward a practical perceptual video quality metric, 2016. [4](#), [13](#)
- [81] Shijie Zhou, Alexander Vilesov, Xuehai He, Ziyu Wan, Shuwang Zhang, Aditya Nagachandra, Di Chang, Dongdong Chen, Eric Xin Wang, and Achuta Kadambi. Vlm4d: Towards spatiotemporal awareness in vision language models. In *Proceedings of the IEEE/CVF international conference on computer vision*, 2025. [3](#), [5](#)
- [82] Tinghui Zhou, Richard Tucker, John Flynn, Graham Fyffe, and Noah Snavely. Stereo magnification: Learning view synthesis using multiplane images. *arXiv preprint arXiv:1805.09817*, 2018. [2](#), [3](#), [7](#), [18](#), [25](#)
- [83] Chen Ziwon, Hao Tan, Kai Zhang, Sai Bi, Fujun Luan, Yicong Hong, Li Fuxin, and Zexiang Xu. Long-lrm: Long-sequence large reconstruction model for wide-coverage gaussian splats. In *Proceedings of the IEEE/CVF International Conference on Computer Vision*, 2025. [7](#)

SpatialVID: A Large-Scale Video Dataset with Spatial Annotations

Supplementary Material

Overview

This supplementary material provides extended details and additional results complementing the main paper. We elaborate on the data curation pipeline (Sec. A), present in-depth analyses of dataset statistics and semantic properties (Sec. B), and describe additional validation tasks and implementation details (Sec. C). An overview of the video filtering and annotation process is shown in Fig. 7.

A. Details of Our Curation Pipeline

Fig. 7 presents the overall data flow of our video curation process, through which the raw videos are progressively refined into the final SpatialVID dataset. The pipeline integrates automatic quality filtering, geometric annotation, and semantic captioning. Figure 8 further illustrates the duration and quantity distribution of the collected raw data, covering diverse indoor and outdoor scenes such as walking, train rides, and drone flights.

A.1. Score Filtering

To ensure data quality, we apply four complementary filters based on *aesthetics*, *luminance*, *text content*, and *motion intensity*. These filters remove visually poor or unsuitable clips before any geometric or semantic processing, significantly improving the robustness of downstream pose estimation.

Aesthetic Filtering. To quantitatively assess visual appeal, we use a CLIP + MLP aesthetic score predictor [47]. The model assigns a score from 0 to 10, with higher values indicating better quality. For each video clip, the score is averaged across the first, middle, and last frames. Clips with an average score below 4.0 are considered insufficiently appealing and discarded (Fig. 9a).

Luminance Filtering. Luminance is calculated for the first, middle, and last frames using the standard formula $L = 0.2126R + 0.7152G + 0.0722B$, where R , G , and B are the respective channel values. Clips with average luminance outside the range [20, 140], either too dark or too bright, are excluded, ensuring that only clips with proper exposure are retained (Fig. 9b).

OCR filter. For text detection, we use the latest release of PaddleOCR [13], which offers high accuracy and robust multilingual support. We process the first, middle, and last frames of each clip to detect text regions, computing the ratio of text area to frame size. Clips where the text area exceeded 30% are removed, as these are considered informational rather than visual (Fig. 9c).

Motion Filtering. We use lightweight VMAF [80],

which is integrated into FFmpeg and outputs a valid motion score ranging from 2.0 to 14.0 (Fig. 9d).

A.2. Geometry Pipeline

We employ **MegaSaM** as our primary geometric reconstruction engine. As shown in Fig. 10, it achieves superior accuracy and robustness compared with DROID-SLAM [53], COLMAP [46], and Fast3R [64], while being faster than MonST3R [74]. Unlike VGGT [55], MegaSaM also maintains stability in feature-sparse scenes. We utilize three trajectory statistics for quality assessment:

Move Distance (MoveDist). Total camera travel distance, computed as the sum of Euclidean distances between consecutive camera centers.

Rotation Angle (RotAngle). Cumulative angular displacement across frames, capturing the extent of viewpoint change.

Trajectory Turns (TrajTurns). Number of significant turns, estimated by counting local extrema in the sequence of orientation angles relative to a start–end reference direction.

A.3. Caption Pipeline

The captioning process integrates visual-language reasoning and structured text generation in two stages.

Stage 1: Visual Parsing. We use Gemini-2.0-flash [51] to analyze sampled frames (1 fps), producing an initial description of camera motion and a summary of scene layout. The prompting format is illustrated in Fig. 11.

Stage 2: Language Refinement. The outputs, along with calibrated camera poses, are then refined using Qwen3-30B-A3B [63]. This stage yields (1) concise scene abstracts, (2) immersive shot-level narratives, and (3) structured semantic tags describing scene type, lighting, weather, crowd density, and time of day. Additionally, *Motion Trends* labels (e.g., pan, dolly, rotate, steady) summarize camera dynamics. Distributions of these tags are shown in Fig. 14. The prompt template used for the large-language refinement is shown in Fig. 12.

A.4. Instruction Examples

Examples of motion instructions are illustrated in Fig. 13. Each instruction corresponds to a specific type of camera movement derived from pose dynamics, providing an interpretable bridge between geometric motion and textual representation. The visualizations demonstrate how camera translations and rotations are systematically mapped to human-readable motion terms, ensuring clarity and consistency across clips.

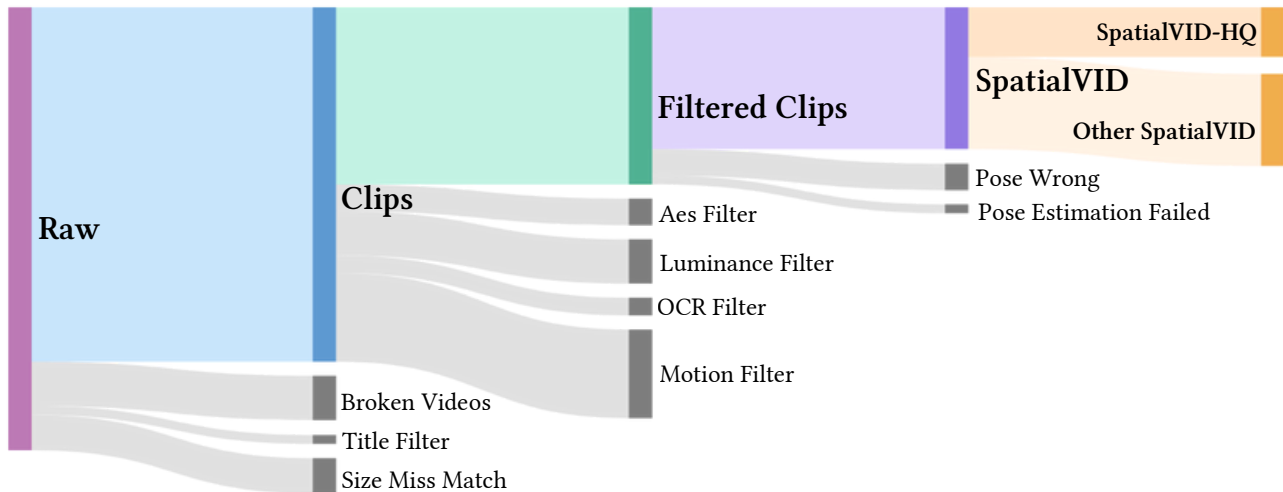


Figure 7. **The data flow of video filtering.** Raw videos are first pre-filtered to exclude content with quality defects, incorrect dimensions, or irrelevant titles. The remaining videos are segmented into clips, which are then ranked via a hierarchical scoring strategy integrating aesthetics metrics, luminance, OCR, and motion values. High-scoring clips undergo a dual annotation pipeline to capture both spatial structure and semantic information, yielding the final SpatialVID dataset. This pipeline is also employed to curate a high-quality subset (SpatialVID-HQ) with a more balanced category distribution.

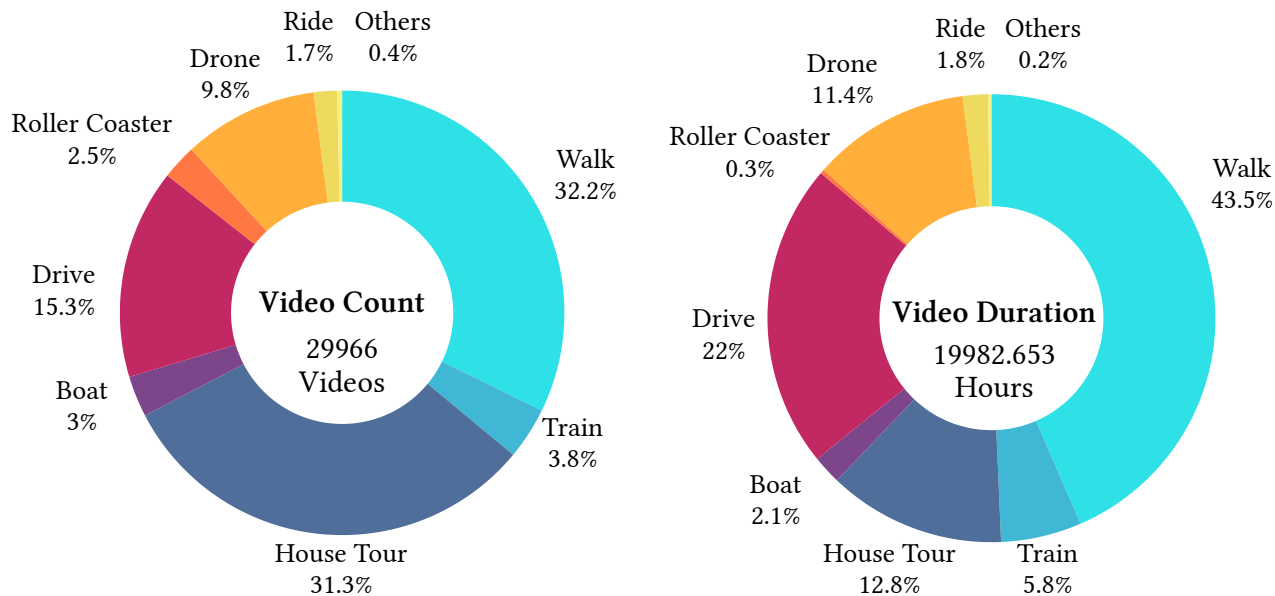


Figure 8. **Statistics of pre-filtered videos** (aka. the “Clips” in the Fig. 7). The left panel shows the quantity distribution of raw videos, while the right panel presents the duration distribution. These charts illustrate the variety of shooting contexts, including indoor (house tour) and outdoor (walking, train, drone, etc.) scenarios, demonstrating broad coverage of different shooting carriers and environments.

B. Details of Dataset Analysis

This section provides extended analyses of the SpatialVID dataset, focusing on semantic composition, caption statistics, and qualitative examples. We examine the distributions of camera motion and scene attributes, analyze caption diversity, and visualize representative samples from the dataset.

B.1. Semantic Analysis

Camera Motion Distribution. Fig. 14 shows the distribution of camera motion directions across SpatialVID and its high-quality subset, SpatialVID-HQ. The original dataset contains a wide range of motion types, including forward, lateral, and rotational movements, but their distribution is not well-balanced. In contrast, SpatialVID-HQ displays a

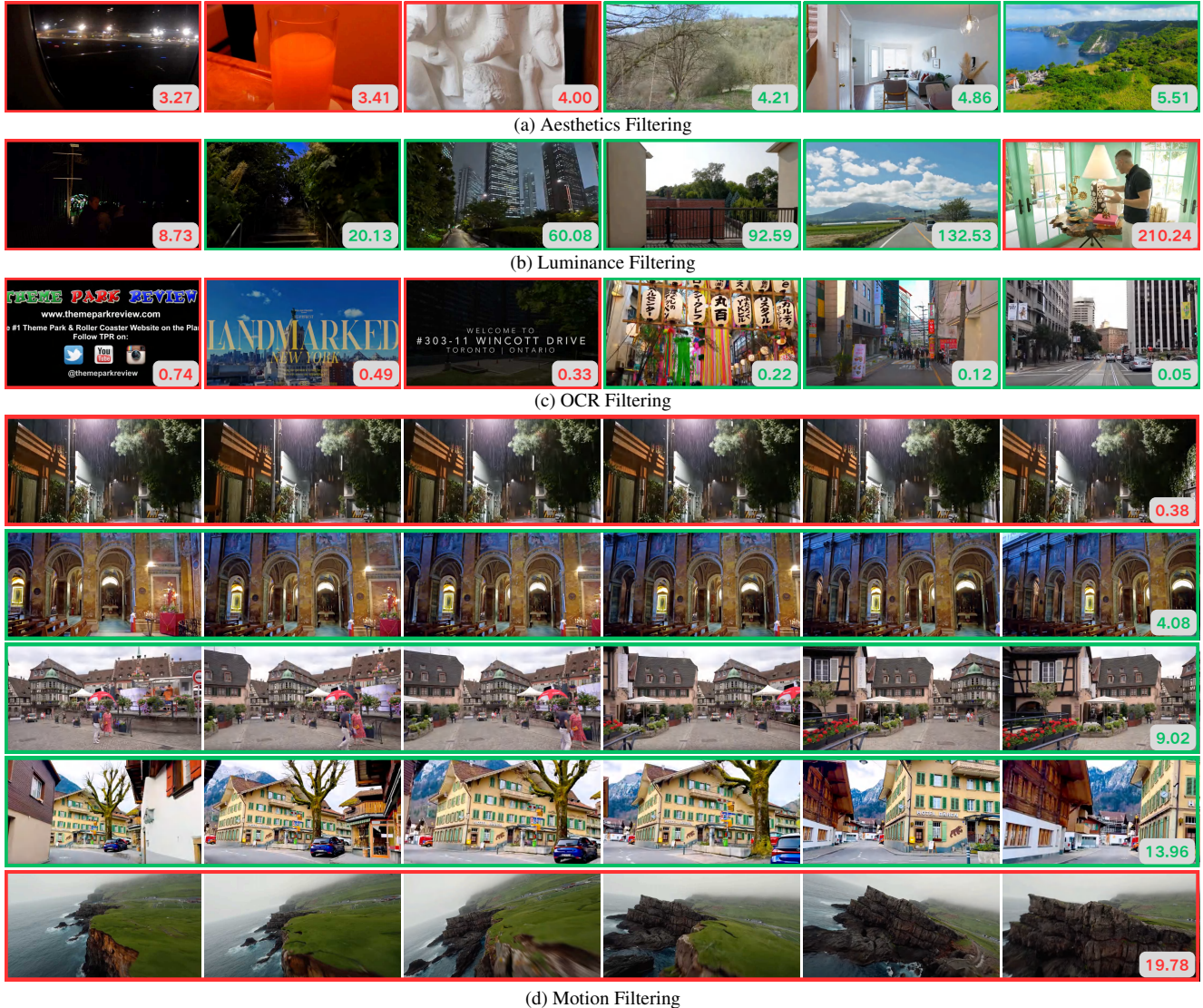


Figure 9. **Video filtering strategies.** Videos are filtered based on various quality criteria (*Aesthetics*, *Luminance*, *OCR*, and *Motion*). The number in the bottom-right corner of each clip represents its score for the corresponding quality filter. Clips with green boxes are retained, while those with red boxes are discarded due to scores below the threshold.

more balanced distribution, mitigating bias toward any single motion direction and offering improved diversity for motion-conditioned generation or control tasks.

Caption Length and Enrichment. We provide multi-level captions for each video, including motion-oriented descriptions, concise scene summaries, and immersive narratives. To evaluate caption quality, we compare the length distributions of original and enhanced captions (Fig. 15). Both motion and scene captions show notable length increases after refinement, reflecting richer context and more detailed spatial reasoning introduced by our LLM-based generation process.

Hierarchical Scene Tags. Fig. 16 visualizes the struc-

tured semantic attributes extracted from enhanced captions. The sunburst chart summarizes the distribution of five primary attributes—weather, time of day, crowd density, lighting, and scene type. The hierarchical scene-type branch covers fine-grained subcategories such as *street*, *park*, *interior*, and *vehicle*. The accompanying word cloud, shaped into the SpatialVID logo, highlights the dataset’s emphasis on spatial and motion-oriented vocabulary, with frequently occurring terms like *motion*, *forward*, and *left*.

Multi-Level Caption Design. SpatialVID delivers a versatile caption suite suitable for various research needs: (1) *OptCamMotion* provides concise, machine-friendly kinematic instructions, reducing average caption length

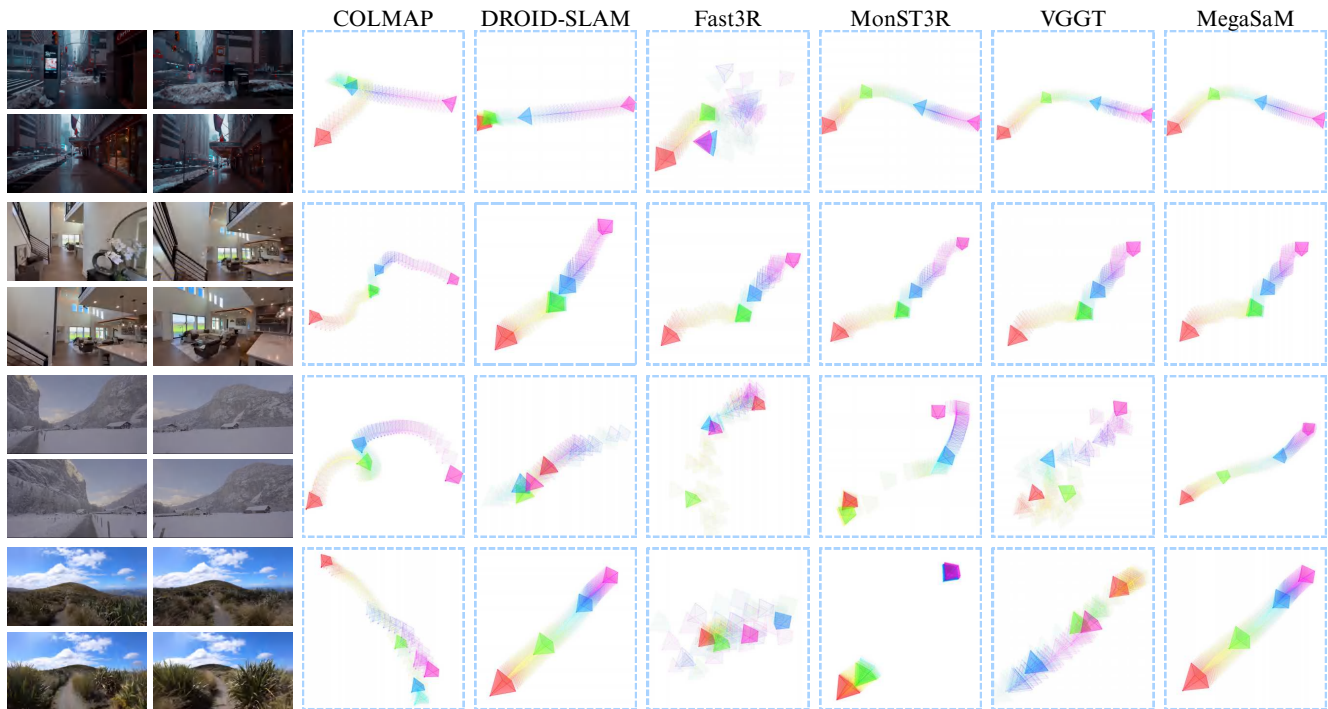


Figure 10. **Comparison of MegaSaM with other SLAM/3D reconstruction methods.** We visualize the trajectories predicted by six representative methods. The color order ROYGBV corresponds to the progression from the initial to the final time step.

You are given a sequence of video frames in chronological order. Analyze them carefully and generate two distinct captions based on the following instructions:

1. Camera Motion Caption:

From the perspective of the camera operator, describe the entire motion trajectory of the camera throughout the clip using precise cinematography terminology (e.g., static, pan, tilt, dolly, handheld, crane, aerial, zoom, etc.).

Do NOT assume the camera starts in a "static" position just because it appears stationary in the first frame. Only describe the camera as stationary if there is no visual change across multiple consecutive frames.

Instead, focus on changes between frames to infer movement. Describe motion state transitions, not frame-by-frame repetition (e.g., do not say "the camera moves forward again" if it's continuous). For example:

- Starting with a dolly forward along a straight path,
- Then transitioning into a slow right-hand pan,
- Or shifting from handheld walking movement to a stationary pivot tilt.

Include brief environmental context where relevant to clarify direction or intent (e.g., "The camera dollies forward through a narrow alleyway, then smoothly turns left at the intersection").

Keep the final caption concise, between 50–100 words, focused only on motion and its evolution over time.

2. Scene Description:

Provide a rich, holistic description of the visual content. Include:

- Main subjects and dynamic objects: who or what is present, and what they are doing (e.g., a cyclist rides past from left to right, a group of people gather near a bench),
- Background/environment: setting (urban street, forest trail, indoor space), notable landmarks or structures,
- Lighting and atmosphere: time of day, weather conditions, mood (e.g., golden-hour lighting, overcast sky casting soft shadows, neon-lit nighttime scene),
- Overall tone or emotion conveyed by the scene.

Avoid focusing on individual frames—describe the general impression and ongoing activity across the entire clip. Aim for around 100 words, balancing detail and conciseness.

Output Format:

Do not include any explanations or extra text before or after your response.

Begin directly with:

1. Camera Motion Caption: ... followed by
2. Scene Description: ...

Figure 11. **Visual-language model (VLM) prompt.** The template guides Gemini-2.0-flash to describe both the visual content and coarse camera motion in natural language, enabling structured parsing of dynamic scenes.

from 62.5 to 50.3 words for clean motion supervision. (2) SceneSummary offers compact high-level context with an average of 28.6 words. (3) ShotImmersion integrates

scene semantics and camera motion into rich narratives averaging 89.7 words, supporting reasoning-intensive tasks such as video understanding and story grounding.

You are given a video sequence with camera trajectory data representing the camera's movement through a scene.

The data consists of:

Camera Motion Caption: A basic description of how the camera moves.

Scene Description: A detailed visual summary of the environment.

Camera position data: Three lines, representing the sequence of the camera's x-coordinate, y-coordinate, and z-coordinate. These values are derived from normalized 3D pose data using the following formula: $\text{poses} = \text{np.round}(\text{poses} / (\text{max_value} - \text{min_value}) / \text{min_abs_value}).\text{astype}(\text{int})$; Each value is then multiplied by 1,000,000 and rounded to the nearest integer.

Motion intensity: An integer that indicates the level of camera movement, where a value of 0 means the camera is static, 1 indicates slight movement, and 2 or higher represents normal or noticeable motion. In tasks such as Optimized Camera Motion Caption and Main Motion Trend Summary, this intensity value should be used to qualify the degree of motion described – for example, using "slight forward translate" when the intensity is 1.

Your Tasks:

1. Optimized Camera Motion Caption

Generate a refined motion caption **from the perspective of the camera itself**, using only the **camera position data** to determine movement direction and dynamics.

Use the following rules to interpret motion:

- x increasing: camera moves right
- x decreasing: camera moves left
- y increasing: camera moves down
- y decreasing: camera moves up
- z increasing: camera moves forward
- z decreasing: camera moves backward

Analyze the full trajectory over time to capture acceleration, deceleration, or steady motion. Integrate scene context but prioritize accuracy based on numerical data. Avoid vague phrases like "zoom out" unless it's clearly due to focal length change – here, use translation terms instead.

If motion intensity is 0, describe the fixed viewpoint and what the camera observes from that vantage point, incorporating compositional or environmental elements from the original caption. If intensity is 1, reflect subtle movement in the description (e.g., "slight right translate") without exaggerating the motion. For both cases, preserve visual context while aligning with the actual movement level. Avoid mentioning data analysis or detection explicitly – let the description itself reflect the motion state.

Target Length: 50–100 words

2. Scene Abstract Caption

Provide a single-sentence summary that captures:

- Key architectural elements
 - Overall atmosphere/style
 - Notable design features
- Target Length: About 50 words

3. Main Motion Trend Summary

Summarize the general movement using only 1–3 short motion phrases, depending on how many are clearly present. Focus strictly on major, sustained movements – ignore minor fluctuations or brief directional changes. If only one or two movements dominate, list only those. Use directional translation terms (e.g., forward translate, left translate, upward drift)

4. Scene Keywords

Extract up to 4 keywords summarizing the key aspects of the scene. Include one term that broadly describes the scene type. Use nouns/noun phrases related to weather, place, time, lighting, scene type. Avoid adjectives/gerunds except for weather. Example: sunset, foggy, marketplace, city street, village

5. Immersive Shot Summary

Blend Optimized Camera Motion Caption and Scene Description evenly – do not focus more on the camera or the scene alone. Describe the visuals as if someone is watching a moving image unfold. Use descriptive, cinematic language that evokes imagery and emotion. Keep it concise but expressive – suitable for use in scripts, storyboards, or AI video/image generation. Target Length: 50–100 words

Given Information:
[VQA Captions]

Camera Position Data:
[Camera Poses]

Output Format:

1. Camera Motion Caption:

[From the perspective of the camera holder, with the camera as the subject. Combine camera pose information to describe]

2. Scene Abstract Caption:

[A concise one sentence summary of the scene]

3. Main Motion Trend Summary:

[keywords separated by commas, e.g., forward translate, downward tilt]

4. Scene Keywords:

[word1, word2, word3, ...] (max 5 words)

5. Immersive Shot Summary

Figure 12. **Large-language model (LLM) refinement prompt.** This instruction template conditions Qwen3-30B-A3B to generate coherent, attribute-rich captions aligned with the extracted spatial and motion cues.

Overall, this structured annotation design ensures both interpretability and flexibility, enabling downstream applications ranging from camera control to multimodal spatial reasoning.

B.2. Examples of SpatialVID

We present qualitative examples in Fig. 17. The selected clips illustrate diverse motion trajectories, scene contexts, and annotation richness. Each sample contains synchronized geometry, caption, and metadata, demonstrating the spatial and semantic consistency maintained throughout the dataset.

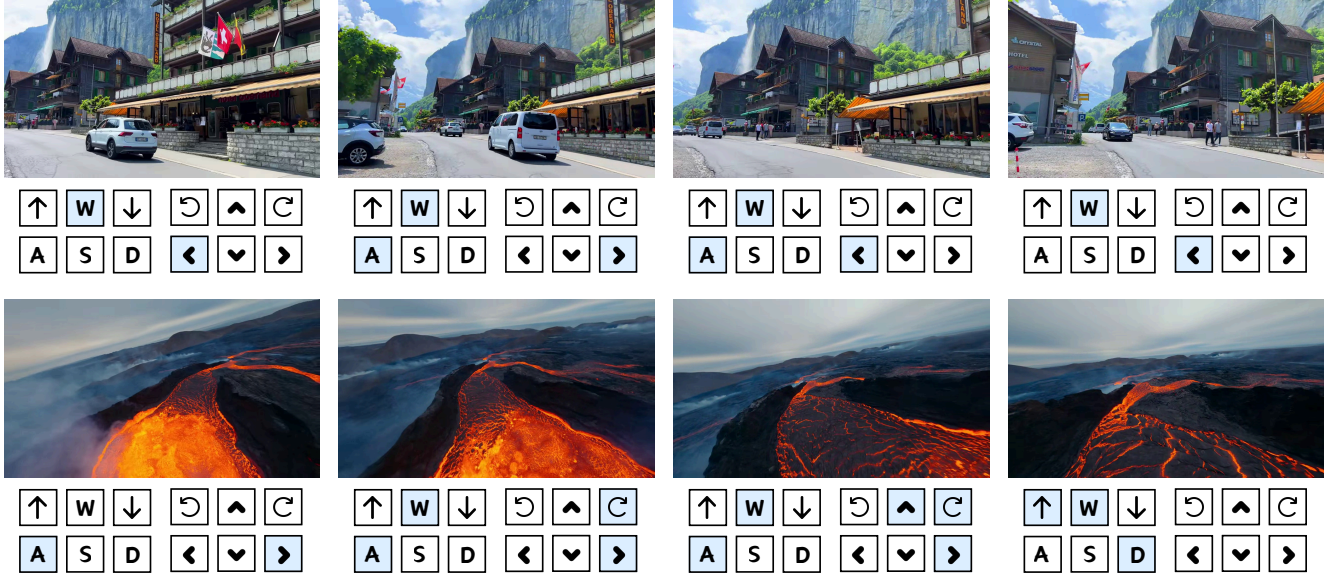


Figure 13. **Examples of motion instructions.** Keyboard-style icons denote camera motion directions. The cluster on the left corresponds to translations: **W** and **S** indicate forward and backward movement, **A** and **D** indicate left and right movement, and \uparrow, \downarrow represent vertical movement. The cluster on the right corresponds to rotations: arrows denote pitch (\wedge, \vee) and yaw (\leftarrow, \rightarrow), while circular arrows indicate roll (\odot, \ominus). These visual cues intuitively describe camera operations, linking geometric motion to semantic labels.

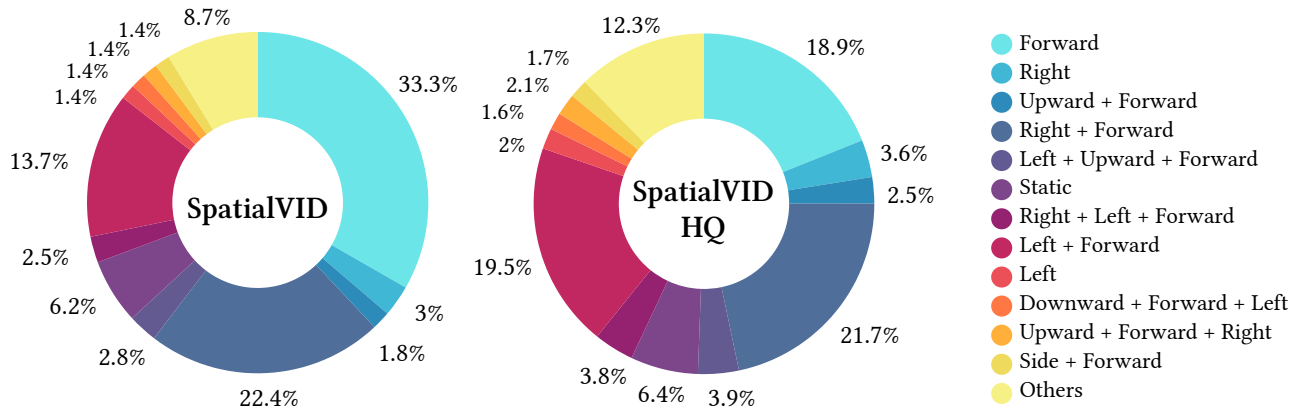


Figure 14. **Distribution of camera motion directions.** The donut charts show the distribution of camera motion directions for the SpatialVID (left) and HQ SpatialVID (right) datasets. The original SpatialVID dataset exhibits a wide range of motion patterns. In contrast, the HQ SpatialVID dataset features a more balanced distribution, addressing the overrepresentation of any single motion direction.

C. Validation Tasks

This section presents the implementation details and qualitative results of validation tasks conducted using the SpatialVID dataset. We focus on three representative paradigms, camera-controlled video generation, spatial reconstruction, and view-consistent rendering, to demonstrate the utility and quality of SpatialVID annotations.

C.1. Implementation Details

Camera-Controlled Video Generation. Experiments are conducted on Sekai-Real [31], RealEstate10K [82], and our SpatialVID-HQ dataset. Since RealEstate10K does not in-

clude textual annotations, we adopt the text captions provided by CameraCtrl [17]. For fair comparison, we follow the original train/test split for RealEstate10K, randomly sample 10K training clips from Sekai-Real, and use all high-quality clips from SpatialVID-HQ. For SpatialVID-HQ, the training captions are derived from the *Immersive Shot Summary* component of our structured annotations. The DiT-based models are initialized from the publicly released T2V-Wan2.2-5B checkpoint [54], ensuring consistent architecture and capacity across datasets. During training, the camera encoder, projector, and self-attention modules are learnable, while all remaining components are frozen. LIn-

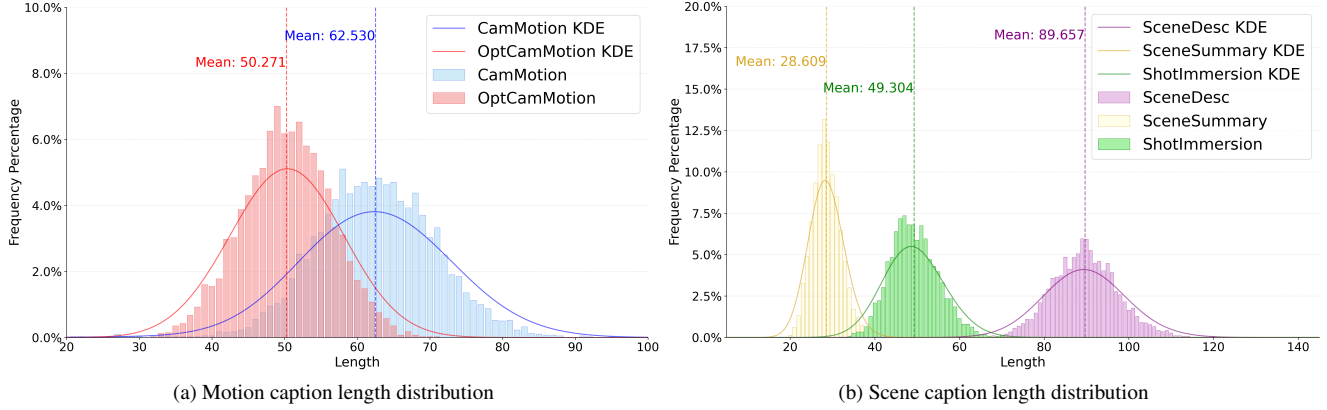


Figure 15. **Statistical analysis of the caption data.** Fig. (a) and Fig. (b) show the length distributions for motion and scene captions, respectively, comparing the original captions to our enhanced versions. A significant increase in caption length is evident for both types after enhancement.

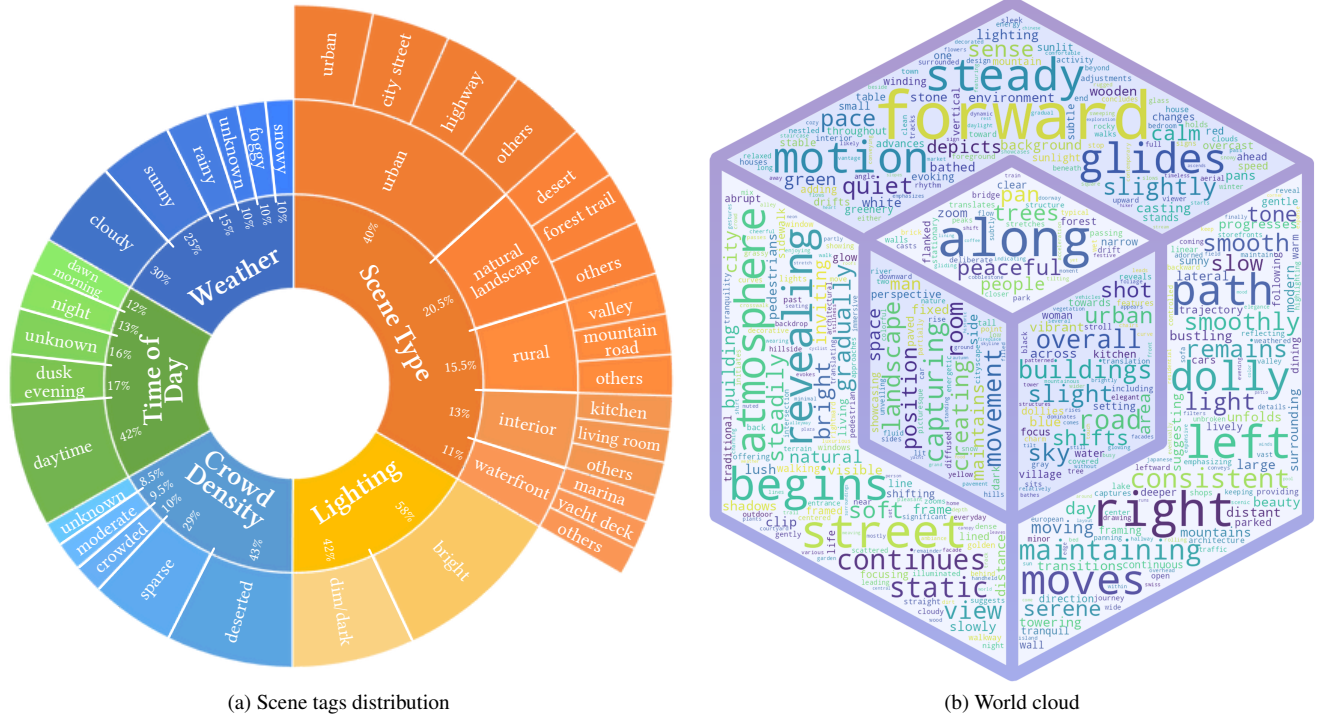


Figure 16. **(a) Distribution of scene tags.** The sunburst chart shows the distribution of categorical tags across five primary attributes: weather, time of day, crowd density, lighting, and scene type. The *scene type* attribute is hierarchical, with sub-categories for more detailed classification. The width of each sector reflects the prevalence of the corresponding tag in the dataset. **(b) Word cloud.** A word cloud shaped into the SpatialVID logo, generated from the enhanced captions. The size of each word corresponds to its frequency in the corpus. Key terms such as *motion*, *forward*, *left*, and *right* emphasize the dataset’s focus on describing camera movement and spatial dynamics.

put frames are resized to 382×480 with a sequence length of 81 frames. We train for 20K steps using a global batch size of 32, the AdamW optimizer with an initial learning rate of 1×10^{-5} , a cosine decay schedule, and a warm-up period of 2K steps. Unless otherwise specified, camera conditioning follows the injection scheme introduced in Re-CamMaster [4]. For each frame, the 3×4 camera extrinsic

matrix (12 parameters) is passed through a learnable linear layer $\text{cam_encoder} \in \mathbb{R}^{12 \times d}$ to project it into the feature dimension d . The resulting embedding is combined with visual tokens through a lightweight per-block *projector* ($\mathbb{R}^{d \times d}$) initialized as an identity mapping to preserve the pretrained feature scale.

CUT3R Fine-tuning. We follow the official fine-tuning

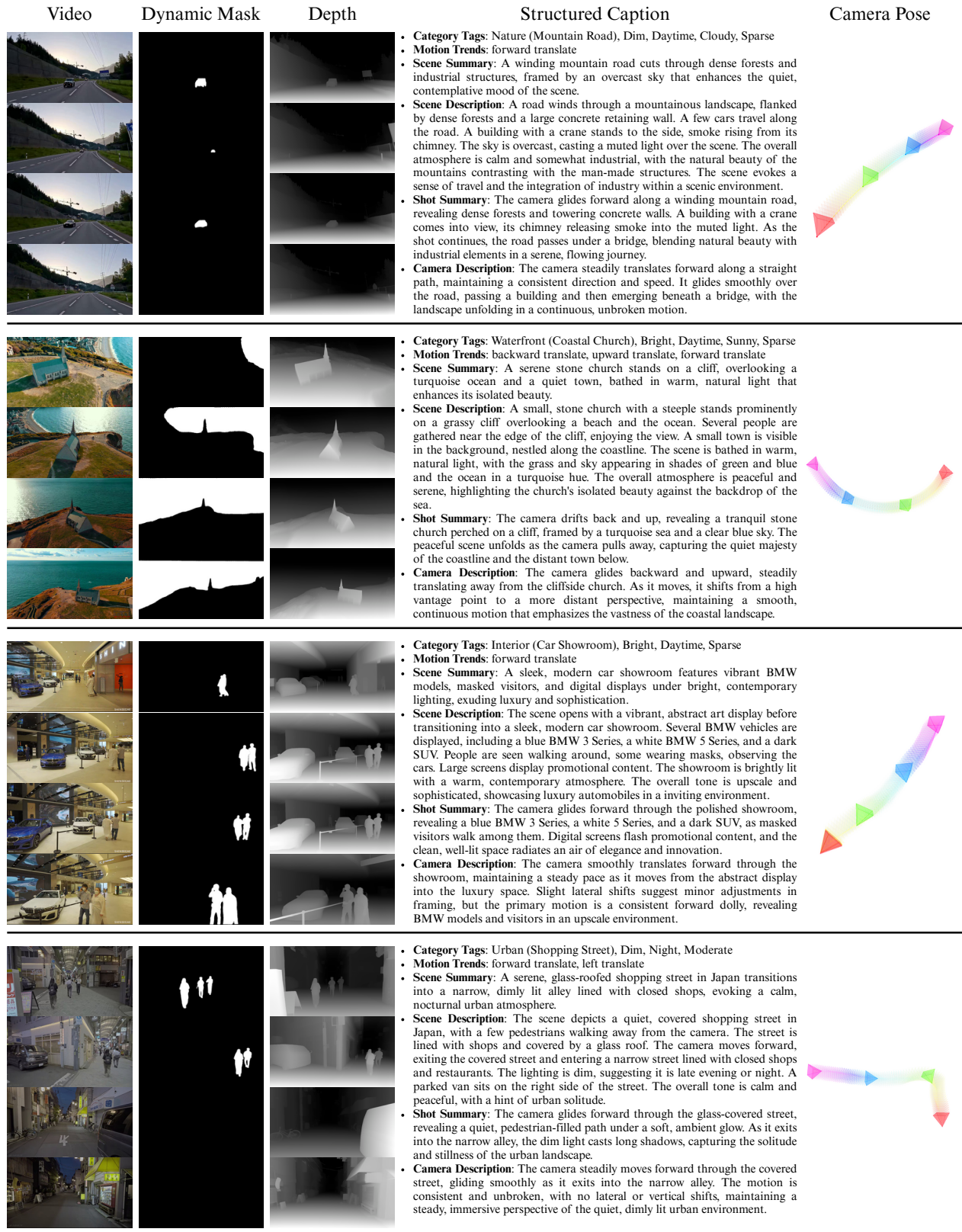


Figure 17. Sample videos from SpatialVID. Each example includes synchronized geometry, captions, and spatial annotations. The dataset encompasses diverse environments and camera motions, highlighting its broad coverage and multimodal consistency.

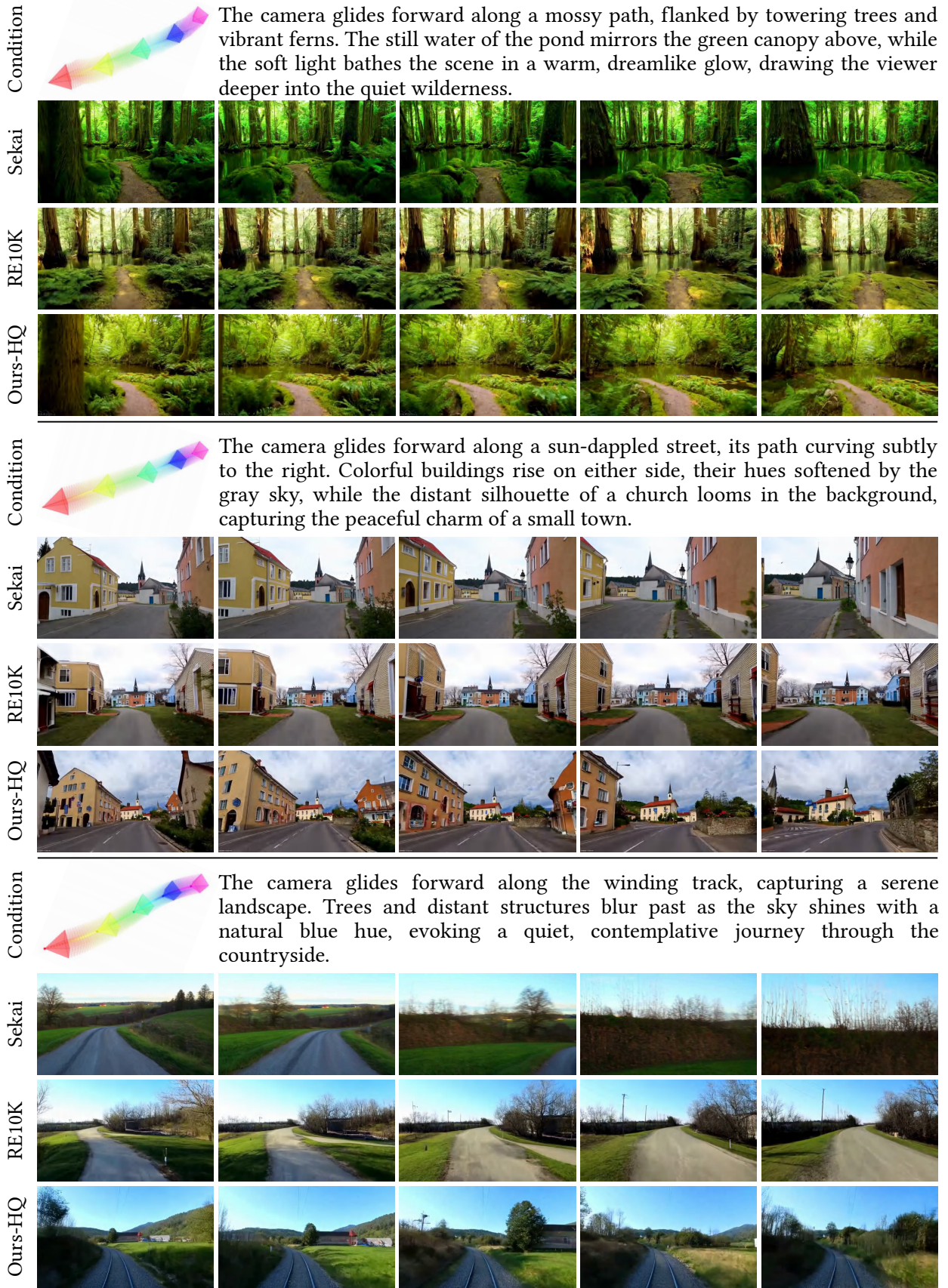


Figure 18. Different training datasets performance on SpatialVID samples.



Figure 19. Different training datasets performance on RealEstate10K samples.



Figure 20. Different training datasets performance on Sekai-Real samples.

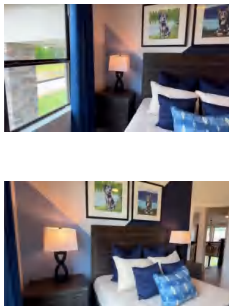
Input Images	GT & Outputs				
	GT				
	SVID				
	R10LK				
	GT				
	SVID				
	R10LK				
	GT				
	SVID				
	R10LK				
	GT				
	SVID				
	R10LK				

Figure 21. GS-LRM qualitative comparison on SpatialVID.

protocol of CUT3R [57] and initialize from the publicly released `cut3r_512_dpt_4_64` checkpoint. Training is performed with a global batch size of 64 using the AdamW optimizer with a learning rate of 1×10^{-6} , a weight decay of 0.05, and a total of 6,500 iterations. We fine-tune on long video sequences ranging from 4 to 64 frames, with each frame resized such that the longer side does not exceed 512 pixels. During training, the encoder is kept frozen while the decoder and output heads are updated to better align CUT3R’s geometric predictions with the spatially consistent captions and camera poses provided by SpatialVID.

VGGT Fine-tuning. We fine-tune VGGT [55] on SpatialVID-HQ together with most of its original training data. For fair comparison, an additional model is fine-tuned using the same original data without SpatialVID-HQ. We initialize from the publicly released VGGT checkpoint and follow the original training strategy, keeping the DINO backbone frozen to ensure consistent architecture and capacity. Training is performed for 40K steps, using the AdamW optimizer with an initial learning rate of 2×10^{-4} . Unless otherwise specified, all remaining hyperparameters follow the default VGGT configuration.

Large Reconstruction Models. All experiments are conducted on RealEstate10K [82] and our SpatialVID-HQ dataset. For fair comparison, both datasets are trained with an equal amount of 60K video clips. In each epoch, random image pairs are sampled, using two views as input and four intermediate views as supervision. All models are trained from scratch to ensure consistent architecture and capacity. Following the GS-LRM [75] training protocol, we adopt a two-stage schedule: the first stage trains at a resolution of 180×320 for 15K steps, followed by a high-resolution stage at 360×640 for an additional 45K steps, totaling 60K steps. Training is performed with a global batch size of 32 using the AdamW optimizer, an initial learning rate of 2×10^{-5} , a cosine decay schedule, and 2K warm-up steps. Unless otherwise specified, the total loss combines pixel-level, perceptual, and depth-smoothness objectives: $\mathcal{L}_{\text{total}} = \lambda_1 \mathcal{L}_{\text{mse}} + \lambda_2 \mathcal{L}_{\text{ipips}} + \lambda_3 \mathcal{L}_{\text{reg}}$, where $\lambda_1 = 1.0$, $\lambda_2 = 0.5$, and $\lambda_3 = 0.25$. The regularization term \mathcal{L}_{reg} encourages depth smoothness by penalizing abrupt depth discontinuities.

C.2. Qualitative Results

We provide additional qualitative comparisons of Camera-controlled video generation and Novel View Synthesis. The camera-controlled video generation results (Fig. 18, Fig. 19, Fig. 20) show that the model trained on *SpatialVID-HQ* precisely follows complex camera trajectories while maintaining realistic spatial continuity and dynamic visual coherence. Moreover, the model demonstrates improved prompt understanding, enabling the generation of more accurate and visually convincing environmental details such as trees and

decorations. The novel view synthesis results (Fig. 21) highlight how SpatialVID supports robust geometry learning, maintaining consistent spatial layouts and detailed texture synthesis across diverse motion trajectories.

By integrating explicit 3D motion control with rich textual semantics, SpatialVID endows physically grounded video generation, dynamic scene synthesis, and spatial intelligence tasks with robust 3D inductive biases. Comprehensive experimental results validate SpatialVID’s effectiveness across diverse tasks, laying a solid foundation for research in the field of spatial intelligence.